의학박사 학위논문

Regulation of histone deacetylase 8 degradation by cAMP signaling system in lung cancer cells

cAMP 신호전달계가 폐암세포주에서 HDAC8 단백질분해를 조절하는 기전

2017 년 2 월

서울대학교 대학원

의과학과 의과학전공

박 지 연

A thesis of the Degree of Doctor of Philosophy

cAMP 신호전달계가 폐암세포주에서 HDAC8 단백질분해를 조절하는 기전

Regulation of histone deacetylase 8 degradation by cAMP signaling system in lung cancer cells

February 2017

The Department of Biomedical Sciences,

Seoul National University

College of Medicine

Ji-Yeon Park

cAMP 신호전달계가 폐암세포주에서 HDAC8 단백질분해를 조절하는 기전

지도교수 전 용 성

이 논문을 의학박사 학위논문으로 제출함
2016년 10월

서울대학교 대학원
의과학과 의과학전공
박 지 연

박지연의 의학박사 학위논문을 인준함
2016년 12월

위 원 장 _____ (인)
부위원장 _____ (인)
위 원 _____ (인)
위 원 _____ (인)
위 원 _____ (인)

Regulation of histone deacetylase 8 degradation by cAMP signaling system in lung cancer cells

by
Ji-Yeon Park

A thesis submitted to the Department of Biomedical Sciences in partial fulfillment of the requirements for the Degree of Doctor of Philosophy in Medical Science at Seoul National University College of Medicine

December 2016

Approved by Thesis Committee:

Professor _____ **Chairman**

Professor _____ **Vice chairman**

Professor _____

Professor _____

Professor _____

Abstract

Regulation of histone deacetylase 8 degradation by cAMP signaling system in lung cancer cells

Ji-Yeon Park
The Department of Biomedical Sciences
The Graduate School
Seoul National University

Histone deacetyalses (HDACs) are enzymes that remove acetyl groups from histones and other proteins and involved in epigenetic regulation of gene expression. Cyclic AMP (cAMP) signaling system is activated by cAMP formed by adenylate cyclases and regulates various cellular functions including gene expression, proliferation and apoptosis. However, the effect of the cAMP signaling system on HDACs has not been studied extensively. This study investigated how the cAMP signaling system regulates HDAC8 expression and its effects on apoptosis in human non-small cell lung cancer (NSCLC) cells.

Activation of cAMP signaling by isoproterenol or prostaglandin E2 (PGE2) increased the HDAC8 expression. Treatment with the exchange protein activated by cAMP (Epac)-selective 8-pCPT-cAMP increased the HDAC8 expression. Inhibition of Epac2 blocked the isoproterenol-induced HDAC8 expression, but the inhibition

of PKA or Epac1 did not block the isoproterenol effect. Isoproterenol and 8-pCPT-cAMP activated Rap1, and Rap1A activation increased HDAC8 expression. Moreover, inhibition of Rap1A abolished the isoproterenol-induced increase in HDAC8 expression. Isoproterenol inhibited Akt by activation of Rap1A, and inhibition of PI3K/Akt activity led to a decrease in the MKK4/JNK pathway and an increase in HDAC8 expression. Activation of cAMP signaling increased HDAC8 protein expression without an increase in HDAC8 mRNA. Inhibition of proteasomal or lysosomal degradation abolished the increase in HDAC8 expression induced by isoproterenol or an Akt inhibitor. Activation of cAMP signaling inhibited autophagy and the ubiquitin-proteasome system and blocked HDAC8 degradation. cAMP signaling decreased the phosphorylation of Bcl-2, and Itch by inhibiting JNK activation, thereby reducing autophagy and the ubiquitin-proteasome system. Isoproterenol augmented cisplatin-induced apoptosis by increasing HDAC8 expression. Exogenous HDAC8 expression reduced the cisplatin-induced TIPRL expression, and knockdown of TIPRL expression augmented the cisplatin-induced apoptosis. The knockdown of HDAC8 restored the cisplatin-induced TIPRL expression and abolished the isoproterenol-induced augmentation of apoptosis. Isoproterenol repressed TIPRL gene transcription by increasing HDAC8 expression. In conclusion, the cAMP signaling system increases HDAC8 expression by inhibiting protein degradation through Epac2-Rap1A-mediated inhibition of PI3K/Akt-JNK pathways and thereby augments cisplatin-induced apoptosis via HDAC8-dependent repression of TIPRL expression in non-small cell lung cancer cells.

Keywords : Akt, apoptosis, autophagy, cAMP signaling, Epac, HDAC8, JNK, lung cancer, ubiquitin-proteasome sytem

***Student number* : 2011-30627**

Contents

List of figures

Introduction

1. cAMP signaling

1–1. Activation of cAMP signaling

Cyclic adenosine 3',5'-monophosphate (cAMP) signaling is activated by cAMP, the first discovered second messenger. cAMP is formed from ATP by adenylate cyclase and degraded by phosphodiesterases. Stimulatory GTP-binding proteins (G proteins), which is activated by G protein-coupled receptors (GPCRs), stimulates the activity of adenylate cyclase. GPCRs are activated by their appropriate signal such as growth factors, hormones, and neurotransmitters [1-3].

1–2. Effectors of cAMP

cAMP signaling can regulate three main targets: cAMP-dependent protein kinase (PKA), cAMP-regulated guanine nucleotide exchange factors (Epac1 and 2), and cyclic-nucleotide-gated ion channels [1, 4]. cAMP signaling leads to the regulation of cellular responses: Proliferation, metabolism and apoptosis in cancer cells [5, 6].

PKA was found as one of the first protein kinases and is tetramer composed of two catalytic subunits and two regulatory subunits. PKA is activated by the binding of two cAMP molecules to each regulatory subunit, and leads to their dissociation from the catalytic subunits. The free catalytic subunits phosphorylate cAMP response element binding protein (CREB), and the activity of PKA is inhibited by protein kinase inhibitors (PKIs) [4].

Recently, Epac proteins were discovered to be a family of new sensors for cAMP, and activate the Ras superfamily of small G proteins, Rap. Epac proteins contain both an N-terminal regulatory region and a C-terminal catalytic region, and Epac proteins can divide two isoforms: Epac1 and Epac2. Epac1 is expressed in all tissues, whereas Epac2 is limited to expression in its tissue distribution. Epac proteins regulate various cAMP-related cellular functions including cell adhesion, proliferation, differentiation and apoptosis [6].

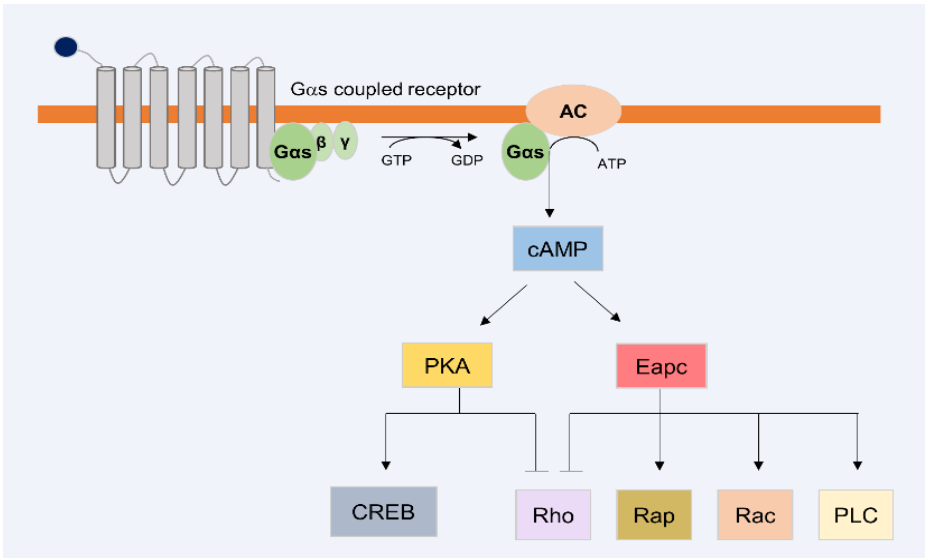

Figure 1. Overview of cAMP signaling [7]

1–3. cAMP signaling and cancer

cAMP singling is one of the important pathways to strategize prevention and treatment in cancer, because it has been found to regulate either positive or negative effects on cell growth, apoptosis, and metastasis, depending on various cancer cell types [8]. In addition, GPCRs which regulate cAMP signaling are overexpressed in

various cancer cells, and the and the aberrant overexpression of GPCRs influences cancer cell growth, angiogenesis and metastasis [9].

2. Histone deacetylases

2–1. Histone deacetylases

Histone deacetylases (HDACs) have been identified as two protein families with HDAC activity: the zinc^{2+}-dependent classical HDAC family, and SIR2 family of NAD^{+}-dependent class III HDACs (SIRT1-7). Classical HDACs may be broadly divided into three subclasses based on their DNA sequence similarity. Class I HDACs (HDAC1, 2, 3, and 8) are related to yeast RPD3, and are expressed in several cell lines and human cancer tissues; class I HDACs are almost located in the nucleus. Class II HDACs (HDAC4, 5, 6, 7, 9, and 10) are homologous to yeast HDA1 and identify tissue–specific expression [10]. These proteins can shuttle between the nucleus and the cytoplasm according to certain cellular signals. Recently, HDAC11 has been discovered as the only class IV HDAC; it has features of both class I and II HDACs, and is localized in the nucleus [11-13].

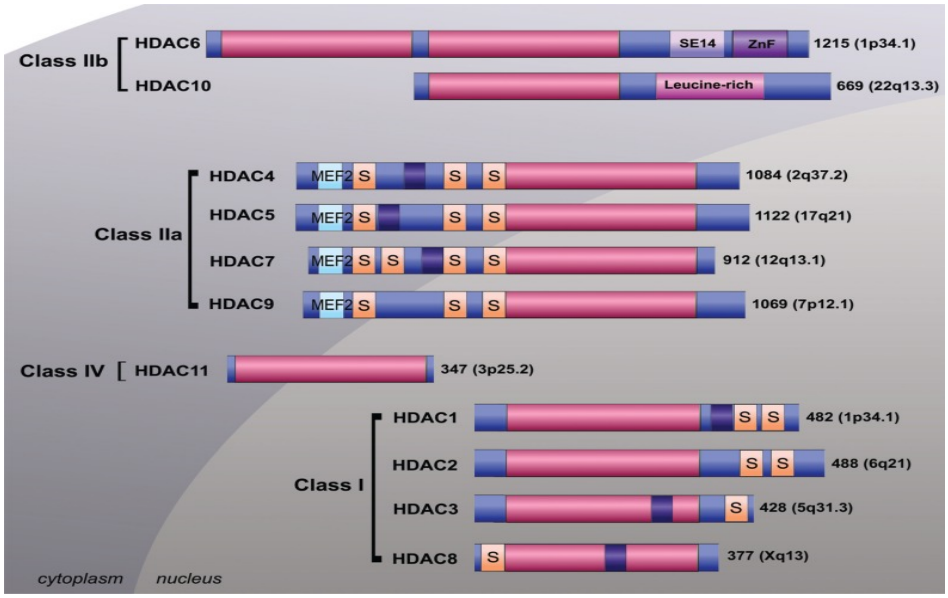

Figure 2. Classification of histone deacetylases (HDACs) [14]

2–2. Histone deacetylase 8 (HDAC8)

Histone deacetylase 8 (HDAC8) is encoded by the HDAC8 gene, and belongs to class I HDACs. The HDAC8 gene is a 377 residue, and is localized on the X chromosome at position q21.2-q21.3, q13. HDAC8 is most closely related to HDAC3, and is found in both the nucleus and the cytoplasm. HDAC8 mRNA levels are expressed in various human tissue types and tumor cell lines [15]. The phosphorylation of HDAC8 by PKA negatively regulates its activity and leads to hyperacetylation of histone H3 and H4 both *in vitro* and *in vivo* [16]. In addition, HDAC8 phosphorylation prevents a telomerase activator, the human ever-short telomeres 1B protein (hEST1B), undergoing ubiquitin-mediated degradation. HDAC8 has non-histone substrates such as the estrogen-related receptor α (ERRα), inv (16) fusion protein, CREB, and p53 [17-19]. HDAC8 plays important roles in transcriptional regulation and cell proliferation, invasion, and apoptosis.

2–3. HDACs and cancer

The overexpression of individual HDACs is found in various human tumors. For example, colon cancer cells overexpress HDAC2 and HDAC3, gastric cancer cells overexpress HDAC1-3, and neuroblastoma overexpresses HDAC8 [20, 21]. HDACs remove acetyl groups from histones, and create condensed chromatin conformation that blocks access to transcription factors. Consequently, HDACs repress the expression of genes such as tumor suppressors, cell cycle inhibitors, and apoptosis inducers in tumorigenesis [22]. In addition, HDACs perform a crucial role in regulating the expression and activity of proteins that are associated with cancer development and progression. Therefore, the inhibition of HDACs activity using HDAC inhibitors can be beneficial in cancer treatment [23, 24].

3. Apoptosis

3–1. Apoptosis

Apoptosis is the process of programmed cell death (PCD) that occurs in physiological and pathological stimulation. The word of apoptosis is derived from Ancient Greek “ἀπόπτῶσις” and means the falling of leaves from trees in autumn. Apoptosis is the removal of cells without their releasing harmful substances into the surrounding area [25]. Various morphological changes occur during apoptosis; for example, cell shrinkage, blebbing, chromatin condensation, chromosomal DNA fragmentation, and nuclear fragmentation. Furthermore, several biochemical changes involving caspase activation, DNA and protein breakdown, and phagocytic recognition can be found in apoptosis. Apoptosis plays a crucial role in tissue

homeostasis and normal development [26, 27].

3–2. Mechanisms of apoptosis

The mechanisms of apoptosis are a disordered process that includes an energy-dependent cascade of molecular events. The apoptotic pathways can be divided two major pathways: The extrinsic death receptor pathway and the intrinsic mitochondrial pathway.

The extrinsic death receptor pathway is initiated by death ligands binding to a death receptor such as the tumor necrosis factor (TNF) receptor gene superfamily, and leads to the ligation of death receptors. As a result, the recruitment of adaptor molecules and the activation of caspase-8 occur. The caspase-8 is an initiator caspase, and its activation triggers executioner caspase-3 and -7 [25].

The intrinsic mitochondrial pathway is initiated by non-receptor-mediated stimuli such as growth factor withdrawal stress, hypoxia, radiation, and the direct effect of the Bcl-2 family proteins, which are regulated by transcriptional and post-transcriptional mechanisms. The Bcl-2 family proteins consist of anti-apoptotic protein (Bcl-2 and Bcl-XL) and pro-apoptotic protein (Bax and Bak), and contain one or more Bcl-2 homology (BH) domains. These proteins govern the mitochondrial outer membrane permeabilization (MOMP), which results in the release of cytochrome-c. The released cytochrome-c activates APAF-1-dependent pro-caspase-9, which then leads to the activation of executioner caspases-3 and -7 [28].

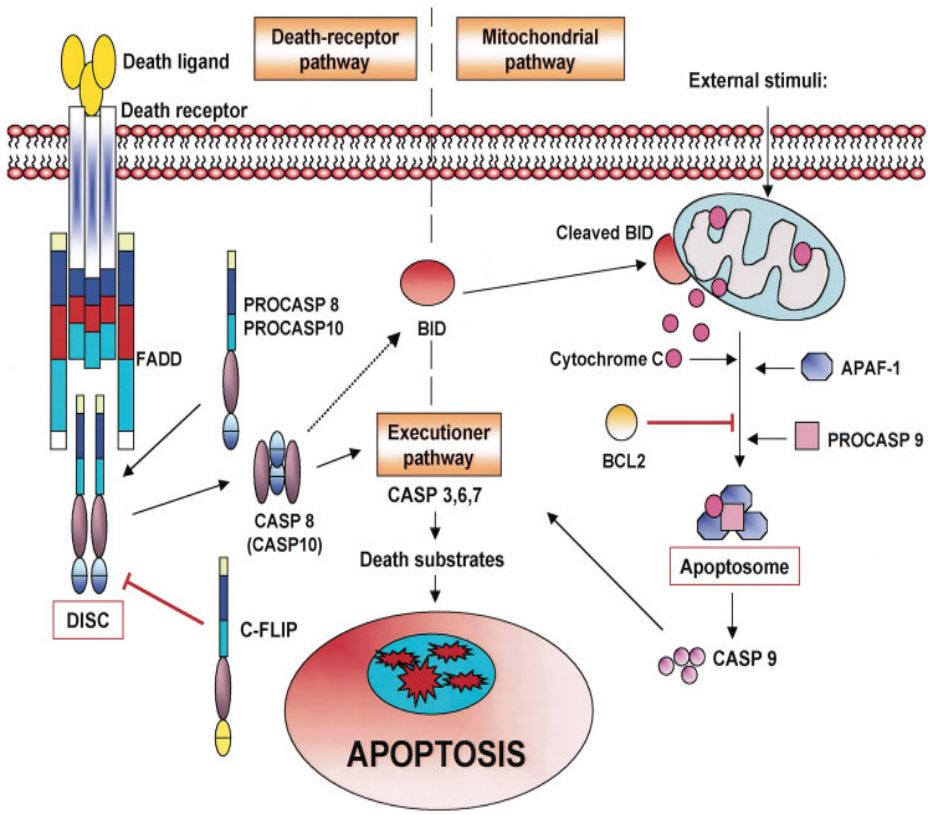

Figure 3. The major pathways to apoptosis [29]

3–3. Apoptosis and lung cancer

Lung cancer leads about one-fifth of all cancer death worldwide. Human lung cancers are divided into two major morphologic groups: Small cell lung cancer (SCLC) and non-small cell lung cancer (NSCLC), and these are regulated by different apoptotic mechanisms depending on the type. The repression of pro-apoptotic proteins and the overexpression or activation of anti-apoptotic proteins is observed in many lung cancers. In particular, NSCLC is less chemo-sensitive compared to SCLC, so it needs targeted therapies such as TNF-related apoptosis-inducing ligand (TRAIL), Bcl-2 family proteins, and apoptosis inhibitory proteins (IAPs) [29, 30].

3–4. cAMP signaling, HDACs and apoptosis

The cAMP signaling system regulates apoptosis either positively or negatively in various cancer cells. In lung cancer cells, the cAMP signaling system stimulates apoptosis by regulating Bcl-2 family proteins and reducing ATM-dependent NF-kB activation, whereas this system inhibits apoptosis by increasing X-linked inhibitor of apoptosis protein (XIAP) in cervical cancer cells and regulating the Bcl-2 family proteins in neuroblastoma cells [31-33].

HDAC inhibitors, known anticancer agents, are able to induce apoptosis via the activation of either an extrinsic or intrinsic pathway in many cancer cells. For example, HDAC inhibitors such as TSA and SAHA downregulate the expression of anti-apoptotic proteins (Bcl-2, Bcl-xL, and XIAP), and increase the expression of pro-apoptotic proteins (Bax and Bak), leading to the stimulation of apoptosis [23, 34].

Purpose

The purpose of this study is to investigate how the cAMP signaling system regulates HDAC8 expression and the effects of resulting increase in HDAC8 on apoptosis in non-small cell lung cancer (NSCLC) cells.

The specific aim of this study was

1. To investigate the singling pathway that mediates cAMP-induced HDAC8 expression in lung cancer cells

2. To investigate the role of autophagy and the ubiquitin-proteasome system in HDAC8 degradation and the mechanism by which cAMP signaling system regulates this degradation

3. To investigate the effect and underlying mechanisms of the resulting increases in HDAC8 expression on cisplatin-induced apoptosis in NSCLC cells

Materials and Methods

1. Cell culture and reagents

Human non-small cell lung cancer cells (H1299 and A549) were purchased from the Korean Cell Line Bank (KCLB, Seoul, Korea). H1299 and A549 cells were maintained in Dulbecco's Modified Eagle's Medium (DMEM) and RPMI 1640, respectively, in a CO_2 incubator at 37°C; the media were supplemented with 10% fetal bovine serum (Welgene, Gyeongsan, Korea) and 100 units/ml penicillin/streptomycin (Welgene). Isoproterenol, H-89, prostaglandin E2, cisplatin, lithium chloride, cycloheximide and dimethylsulfoxide (DMSO) were purchased from Sigma-Aldrich (St. Louise, MO, USA). Isobutylmethylxanthine (IBMX), LY294002, wortmannin, SP600125, PYR-41, and MG-132 were purchased from Calbiochem (Nottingham, UK), and 8-pCPT-2'-O-Me-cAMP and ESI-05 were from Biological Life Science Institute (Bremen, Germany). Ammonium chloride was purchased from Merck Millipore (Billerica, MA, USA), and forskolin was purchased from Cayman (Ann Arbor, MI, USA). MK-2206 was purchased from Selleckchem (Houston, TX, USA). Lipofectamine 2000 was purchased from Invitrogen (Carlsbad, CA, USA).

2. Expression plasmids and transient transfection

The expression plasmid of the EE-tagged constitutively active mutant Gαs (GαsQ227L) in pcDNA3.1(+) vector was purchased from Missouri S&T cDNA Resource Center (Rolla, MO, USA). A dominant-negative mutant of PKA (dnPKA)

was a gift from G. Stanley MecKnight (University of Washington, WA, USA). The green fluorescent protein (GFP)-tagged PKA catalytic subunits (GPKA) was provided by Steven H. Green (University of Iowa, IA, USA). The pRK5 expression vectors encoding constitutively active Rap1A-V12 (caRap1A) and dominant-negative Rap1A-N17 (dnRap1A) were kind gifts from J. O'Neill (Trinity College, Ireland). Wild-type HDAC8 was provided by Jaeku Kang (Konyang University, Daejeon, Korea). A dominant-negative mutant of Akt1 in pUSEamp (dnAkt1) was provided by ByungLan Lee (Seoul National University College of Medicine, Seoul, Korea). A dominant negative mutant of JNK (dnJNK) mitogen-activated protein kinase (MAPK) and a constitutively active mutant of JNK (caJNK) were provided by You Mie Lee (Kyungpook National University, Daegu, Korea) and Pann Ghill Suh (Ulsan National University of Science and Technology, Ulsan, Korea), respectively. The plasmids expressing a short hairpin RNA sequences targeting HDAC8, Epac1, Epac2, Rap1A, and scrambled shRNA (negative control) were purchased from Sigma-Aldrich. Small interfering RNAs (siRNAs) against HDAC8 (cat. sc-35548), Tip41 (TIPRL, cat. sc-78723), AIP4 (Itch, cat. sc-40364) and control siRNA were purchased from Santa Cruz Biotechnology (Dallas, TX, USA). The constructs were expressed by transient transfection using Lipofectamine 2000 (Invitrogen, Carlsbad, CA, USA).

3. Western blot analysis

Western blotting was performed as previously described [35]. The following primary antibodies were used: antibodies against HDAC8, glycogen synthase kinase 3β (GSK-3β), SQSTM1 (p62), Skp2 and MDM2 were purchased from Santa Cruz

Biotechnology; antibodies against cAMP response element binding protein (CREB), p-CREB (S133), p-PKA substrate, Rap1, p-Akt (S473), p-Akt (T308), Akt, p-GSK-3β (S9), p-β-catenin, Myc, Beclin1, Atg5, p-AMPKα (T172), AMPKα, p-mTOR (S2448), mTOR, p-MKK4 (S257), MKK4, p-JNK (T183/Y185), JNK, p-Bcl-2 (S70), Bcl-2, CHIP, LC3B, and p-Mdm2 (S166), poly (ADP-ribose) polymerase (PARP), cleaved caspase-3 and cleaved caspase-9 were purchased from Cell Signaling Technology (Beverly, MA, USA); antibodies against TIPRL and Itch/AIP4 were purchased from Abcam (Cambridge, UK); an antibody against p-Itch was purchased from Merck Millipore; an antibody against β-Actin was purchased from Sigma-Aldrich. The proteins were visualized with the Enhanced Chemiluminescence (ECL) reagent (Thermo Fisher Scientific; Waltham, MA, USA) and detected using an LAS-3000 luminescent image analyzer (Fuji, Tokyo, Japan). The densities of the visualized bands were quantified using the Multi Gauge v.2.3 software (Fuji). The densities were normalized to corresponding control densities and expressed relative to the control.

4. Reverse Transcription Polymerase Chain Reaction (RT-PCR)

Total RNA was isolated from cells using Trizol (Invitrogen). First strand complementary DNA (cDNA) was synthesized using oligo-dT primers and the SuperScript First-Strand Synthesis System (Invitrogen). RT-PCR was performed in a 25 μl mixture with 500 nM forward and reverse primers, and rTaq (Takara Shuzo Co., Otsu, Japan) using a GeneAmp PCR system 2700 (Applied Biosystems, Waltham, MS, SA). PCR thermal cycle parameters were: Denaturation at 95℃ for 5

min, 30 cycles of 94℃ for 1min, 55℃ for 1 min and 72℃ for 1 min, followed by 10 min of extension at 72℃. PCR of GAPDH was performed as a control for RNA quantity. The oligonucleotide primers used in PCR were as follows: Itch; forward primer 5'-CCTTACGTAGAGGTCACAGT-3', reverse primer 5'-CTCCAAGCTGCAAAGTCAC-3', GAPDH; forward primer 5'-ACCACAGTCCATGCCATCAC-3', reverse primer 5'-TCCACCACCCTGTTGCTGTA-3'. RT-PCR products were separated on an agarose gel containing ethidium bromide and visualized by ultraviolet light.

5. Quantitative Reverse Transcription Polymerase Chain Reaction (qRT-PCR)

qRT-PCR was performed in a 20 μl mixture composed of 250 nM forward and reverse primers, and SYBR Ex Taq (Takara Shuzo Co.) using a C1000 thermal cycler (BioRad, Hercules, CA, USA). The PCR parameters were as follows: 30 sec at 95°C followed by 40 cycles of 95°C for 5 sec and 55°C for 31 sec. After 40 cycles, the average threshold cycle (Ct) values from triplicate PCR reactions were normalized against the average Ct values of GAPDH. The qRT-PCR primer sequences were as follows: HDAC8, forward primer 5'-ATCTCAATGATGCTGTCCTGG-3', reverse primer 5'-CATGATCTGGGATCTCAGAGG-3'; TIPRL, forward primer 5'-GCTGTTGCGGTTTTTCTTGA-3', reverse primer 5'-AGAGGGAAGGTGGAACATGC-3'; GAPDH, forward primer 5'-ACCACAGTCCATGCCATCAC-3', reverse primer 5'-TCCACCACCCTGTTGCTGTA-3'.

6. Rap1 activation assay

pGEX Ral GDS-RA, a plasmid for the expression of GST-RalGDS-RBD, was provided by Dr. Jay H. Chung (National Institutes of Health, Bethesda, MD, USA). The plasmid was transformed into *Escherichia coli* (Rosetta strain), and protein expression was induced by adding isopropyl β-D-thiogalactopyranoside (IPTG) to the culture. The bacterial lysate (50 μl per sample) that contained the GST-RalGDS-RBD fusion protein was mixed with glutathione-Sepharose 4B beads (GE Healthcare Life Sciences, Pittsburgh, PA, UAS) for 1 h at 4°C on a rotator. After the beads were washed three times with the lysis buffer (50 mM Tris-HCl, pH 7.5, 150 mM NaCl, 5 mM $MgCl_2$, 1% Nonidet P-40, 5% Glycerol, 1 mM Na_3VO_4, 5 mM NaF, 1 mM PMSF and a protease inhibitor mixture), 500 μg of the cell lysate was added to and mixed with the beads for 1 h at 4°C on a rotator. The beads were washed three times with the lysis buffer. The bound proteins were eluted with 2X loading buffer and boiled for 5 min at 100°C. The eluted proteins were analyzed by western blot.

7. Flow cytometry

H1299 cells were treated with cisplatin (50 μM) and incubated for 48 h. Then, the cells were washed with phosphate-buffered saline and harvested by trypsinization and centrifugation at 500 ×g for 3 min. The cells were incubated in annexin V buffer containing FITC-annexin V and propidium iodide for 15 min in dark. The fluorescence of 10,000 cells per sample was detected with FACSCanto II flow cytometer (BD Biosciences, Franklin Lakes, NJ, USA).

8. Generation of TIPRL-promoter reporter constructs

The forward primer that was designed to clone the TIPRL promoter region included an NheI site at its 5' terminus and contained the following sequence: 5'-CCCGCTAGCTACCTGCAATTCCCAACTCCC-3'. The reverse primers included a HindIII site at its 5' terminus and contained the following sequences: R1; 5'-CCCAAGCTTGGCTGAGGCAGGACCCGCAGA-3' and R2; 5'-CCCAAGCTTGAAGCAGAAATCCCGGTGGCT-3'. PCR was performed with LA Taq polymerase (Takara Shuzo Co), and PCR products were ligated into a T-vector and digested with XcmI. The cloned promoter regions were then subcloned into a pGL2-basic vector (Promega Co., Madison, WI, USA) for the analysis of TIPRL promoter activity. A 935-bp region of the TIPRL promoter was cloned into the pGL2-luciferase vector (TIPRL_R1). Additionally, a 980-bp region of the TIPRL promoter with the ATG region was also cloned into the pGL2-luciferase vector (TIPRL_R2).

9. Dual-luciferase activity assay

H1299 cells were transfected with plasmids that contained luciferase reporter genes (TIPRL_R1-pLuc and TIPRL_R2-pLuc) and the control Renilla-pLuc plasmid using Lipofectamine 2000 (Invitrogen). The Dual-Luciferase Reporter Assay System (Promega Co.) was used to assay the luciferase activities after 24 h according to the manufacturer's instructions. At least three independent experiments were performed in duplicate, and the promoter activity was normalized to the Renilla activity.

10. Data analysis

All experiments were independently repeated at least three times, and the data are presented as the mean ± standard error (SE). The non-parametric Mann-Whitney U test was used to analyze the mean values, and *p*-values < 0.05 were considered statistically significant.

Results

1. cAMP signaling increased HDAC8 expression in non-small cell lung cancer cells

To investigate the effect of cAMP signaling on HDAC8 expression, cAMP signaling was activated by treatment with isoproterenol (a Gαs-coupled β-adrenergic receptor agonist, in H1299 human non-small cell lung cancer (NSCLC) cells. Isoproterenol increased the HDAC8 expression significantly with the highest level at 30 min after treatment, and then the HDAC8 protein level returned to the unstimulated level at 2 h after treatment (Fig. 4). The activation of cAMP signaling by treatment with another Gαs-coupled receptor agonist (PGE2) or adenylate cyclase activator (forskolin) also increased HDAC8 expression, but did not significantly changed HDAC8 mRNA levels in H1299 cells (Fig. 5 and 6). In addition, HDAC8 expression was also increased by the activation of cAMP signaling through expressing GαsQL or treatment with isoproterenol in A549 human NSCLC cells (Fig. 7 and 8). These results show that cAMP signaling increases HDAC8 protein expression in human NSCLC cells.

2. cAMP signaling increased HDAC8 expression via a PKA-independent pathway

To investigate how cAMP signaling increases HDAC8 expression, the role of PKA, the best-known cAMP effector, was assessed. The inhibition of PKA by treatment

with a selective PKA inhibitor (H-89) or by expressing a dominant-negative PKA (dnPKA) did not block the HDAC8-increasing effect of isoproterenol in H1299 cells (Fig. 9 and 10). In addition, the expression of catalytic subunit of PKA (GPKA) did not increase HDAC8 expression significantly, though it increased phosphorylation of many PKA substrates (Fig. 11). These results indicate that the cAMP signaling increases HDAC8 expression via a PKA-independent pathway.

3. Isoproterenol increased HDAC8 expression via the Epac2-Rap1A pathway

To examine the signaling pathway mediating the HDAC8-increasing effect of cAMP, the role of Epac, another cAMP effector, was assessed. The Knockdown of Epac1 using an Epac1-specific shRNA did not block the isoproterenol-induced increase in HDAC8 expression. However, the knockdown of Epac2 by an Epac2-specific shRNA or inhibition of Epac2 with an Epac2-selective inhibitor (ESI-05) abolished isoproterenol-induced increase in HDAC8 expression (Fig. 12-14). Treatment with an Epac-selective agonist (8-pCPT-cAMP) increased HDAC8 expression to a degree similar to that observed in isoproterenol-treated cells (Fig. 15). As a downstream target of Epac2 in isoproterenol-induced HDAC8 expression, the involvement of Rap1A was studied. Because Rap1 is a well-known effector of Epac. Treatment with isoproterenol or 8-pCPT-cAMP caused an increase in GTP-bound Rap1, indicating the increased Rap1 activation (Fig. 16), and inhibition of Epac2 with an inhibitor (ESI-05) abolished the isoproterenol-induced increase in GTP-bound Rap1 (Fig. 17). Rap1A activation by the expression of constitutively active Rap1A (caRap1A) also increased HDAC8 expression (Fig. 18) Moreover, Rap1A inhibition by the

expression of a dominant-negative Rap1A (dnRap1A) or the knockdown with a specific-Rap1A shRNA blocked the isoproterenol-induced increase in HDAC8 expression (Fig. 19 and 20). These results indicate that the cAMP signaling increases HDAC8 expression via Epac2-Rap1A-mediated pathway (Fig. 21).

4. Isoproterenol increased HDAC8 expression by inhibiting PI3K/Akt pathway

To further probe the signaling pathway that mediates the HDAC8-increasing effect of cAMP downstream of Rap1A, we screened signaling pathways including mitogen activated protein kinases (MAPKs) and phosphoinositide 3-kinase (PI3K)/Akt. Treatment with isoproterenol decreased the phosphorylation of Akt, ERK, JNK, and p38 MAPKs (Fig. 22). Next, we addressed whether that Epac-Rap1 inhibits Akt. Treatment with isoproterenol or 8-pCPT-cAMP inhibited Akt phosphorylation at Thr-308 and Ser-473 (Fig. 23). The expression of constitutively active Rap1A also decreased Akt phosphorylation at Thr-308 and Ser-473 (Fig. 24), and knockdown of Rap1A restored Akt phosphorylation from the isoproterenol-induced decrease (Fig. 25). These results suggest that cAMP signaling inhibits the PI3K/Akt pathway in an Epac2-Rap1A-dependent manner.

To investigate the roles of PI3K and Akt in cAMP-induced increase in HDAC8 expression. PI3K inhibition with PI3K inhibitors (LY294002 or wortmannin), or by the expression of dominant-negative PI3K (dnPI3K) increased HDAC8 expression in H1299 cells (Fig. 26 and 27). In addition, Akt inhibition with Akt inhibitor (MK-2206) or by the expression of dominant-negative Akt1 (dnAkt) also increased HDAC8 expression (Fig. 28 and 29) without changing HDAC8 mRNA levels (Fig.

30). Because Akt inhibition results in a reduction of inhibitory phosphorylation and thus activation of GSK-3β, we assayed the role of GSK-3β as downstream pathway of Akt. The inhibition of GSK-3β activity by treatment with CHIR99021, a GSK-3β inhibitor, did not block the isoproterenol-induced HDAC8 expression (Fig. 31), suggesting GSK-3β does not mediate HDAC8 expression. Taken together, these findings indicate that cAMP signaling increases HDAC8 expression via Rap1A-dependent inhibition of the PI3K/Akt pathway (Fig 32).

5. cAMP signaling increased HDAC8 protein levels by inhibiting HDAC8 degradation

Because cAMP signaling increase HDAC8 protein levels but not change HDAC8 mRNA levels, we investigated whether protein biosynthesis was involved in the cAMP-induced increase in HDAC8 protein levels. We assessed the effect of cAMP signaling on HDAC8 expression after blocking protein biosynthesis by treatment with cycloheximide. The analysis showed that isoproterenol and forskolin/IBMX increased HDAC8 protein levels in the cycloheximide-pre-treated cells, indicating that the increase in HDAC8 protein levels induced by cAMP signaling was independent of protein biosynthesis (Fig. 33). Next, we examined the effect of inhibiting protein degradation due to autophagy and proteasome on the cAMP signaling-induced increase in HDAC8 protein levels. Treatment with lysosomal inhibitors (NH_4Cl, chloroquine) or a proteasomal inhibitor (MG-132) increased HDAC8 expression. However, treatment with isoproterenol or MK-2206 failed to cause a further increase in HDAC8 protein levels in the cells pre-treated with

lysosomal or proteasomal inhibitors (Fig. 34 and 35). These findings suggest that cAMP signaling might increase HDAC8 protein levels by inhibiting the HDAC8 degradation that is mediated by both the lysosome and the proteasome systems.

6. cAMP signaling inhibited autophagy-mediated HDAC8 degradation

To confirm that the HDAC8 protein is degraded by autophagy, we analyzed the effect of inhibiting different steps of autophagy on HDAC8 expression. We first analyzed the effect of class III phosphatidylinositol 3-kinases (PI3K) inhibition on HDAC8 expression. Inhibition of PI3K by treatment with 3-methyladenine (3-MA) increased HDAC8 expression (Fig. 36). Next, we examined the effect of blocking Atg5 or Beclin1 on HDAC8 expression. Knockdown of Atg5 or Beclin1 with specific siRNAs increased HDAC8 expression (Fig. 37), and these results showed that inhibition of autophagy at different steps increased HDAC8 expression confirming that autophagy is involved in HDAC8 degradation in H1299 cells.

Then, we examined that the effect of cAMP signaling on autophagy. The activation of cAMP signaling by treatment with isoproterenol increased the p62 protein levels (Fig. 38). The activation of cAMP signaling by the expression of constitutively active Gαs also increased p62 expression (Fig. 39) and reduced the conversion of LC3-I to LC3-II (Fig. 40). Therefore, the accumulation in p62 levels and the reduction in LC3-II levels caused by the activation by cAMP signaling indicate that cAMP signaling inhibits autophagy in H1299 cells.

Next, we examined the involvement of Bcl-2 because Bcl-2 binds to Beclin1 to inhibit autophagy. Treatment with isoproterenol or forskolin/IBMX reduced Bcl-2

phosphorylation at Ser-70 in H1299 cells (Fig. 41). These results indicate that the activation of cAMP signaling might inhibit autophagy by inhibiting Bcl-2 phosphorylation and that cAMP signaling increases HDAC8 expression, in part, by inhibiting the degradation of HDAC8 via autophagy in H1299 cells.

7. cAMP signaling inhibited ubiquitin-proteasome dependent HDAC8 degradation in H1299 cells

To confirm that cAMP signaling affects the ubiquitin-proteasome-dependent degradation of HDAC8, we analyzed the effect of inhibiting the ubiquitin E1 enzyme on HDAC8 expression. The inhibition of E1 enzyme by treatment with PYR-41 increased HDAC8 expression (Fig. 42). This result, together with the proteasome inhibitor study (Fig. 34 and 35), indicates that the HDAC8 protein is degraded via the ubiquitin-proteasome system in H1299 cells. To identify the E3 ubiquitin ligase involved in HDAC8 ubiquitination, we analyzed HDAC8 expression after knocking down the E3 ligases that have been reported to be regulated by cAMP signaling. The expression of HDAC8 was increased in the cells where any one of the E3 ligases (Itch, MDM2, Skp2, or CHIP) were knocked down using specific siRNA or shRNAs, suggesting that all of the E3 ligases examined are involved in HDAC8 degradation (Fig. 43). An additional test to find the E3 ligase that mediated isoproterenol's effects on HDAC8 expression found that the phosphorylation of Itch was reduced by the activation of cAMP signaling with isoproterenol and forskolin/IBMX (Fig 44). However, the expression of the other E3 ligases was not decreased by treatment with isoproterenol, suggesting these E3 ligases do not mediate isoproterenol's effect on HDAC8 degradation (Fig. 45). These results indicate that Itch is the E3 ligase that is

responsible for HDAC8 ubiquitination and mediates the effect of cAMP signaling on HDAC8 degradation in H1299 cells.

8. cAMP signaling reduced the HDAC8 degradation via JNK-mediated inhibition of autophagy and the ubiquitin-proteasome system

To probe how cAMP signaling simultaneously inhibits the HDAC8 degradation via the autophagy-lysosome and ubiquitin-proteasome pathways, we analyzed the role of JNK1 in this process because JNK has been reported to phosphorylate both Bcl-2 and Itch. When cAMP signaling was activated by treatment with isoproterenol and forskolin/IBMX, the activating phosphorylations of JNK and upstream MKK4 were decreased in H1299 cells, suggesting a decrease in JNK activity (Fig. 46). We then investigated the effect of JNK on the phosphorylation of Bcl-2 and Itch. Inhibition of JNK activity by treatment with a JNK inhibitor (SP600125) or by the expression of dominant-negative JNK decreased the phosphorylation of both Bcl-2 and Itch and increased HDAC8 expression (Fig. 47 and 48). However, the expression of a constitutively active JNK abolished the effect of isoproterenol on the phosphorylation of Bcl-2 and Itch (Fig. 49). These results indicate that cAMP signaling inhibits both the JNK-mediated phosphorylation of Bcl-2, thereby reducing autophagy, and the JNK-mediated phosphorylation of Itch, thereby reducing ubiquitin-proteasome-dependent degradation, resulting in increased HDAC8 protein levels.

To identify the pathway by which cAMP signaling inhibits JNK, we examined the role of PI3K and Akt in this process. cAMP signaling has been found to increase HDAC8 protein levels by inhibiting the PI3K/Akt pathway in H1299 lung cancer cells. Isoproterenol treatment decreased the activating phosphorylation of Akt in H1299 cells (Fig. 23). Inhibition of either PI3K or Akt activity by treatment with a PI3K inhibitor (LY294002) or an Akt inhibitor (MK-2206) decreased the activating phosphorylation of JNK1 and the inhibitory phosphorylation of GSK-3β (Fig. 50). These results indicate that cAMP signaling inhibits JNK1 activity by reducing PI3K-Akt activity and suggest that cAMP signaling inhibits the degradation of HDAC8 protein via the PI3K-Atk-JNK-dependent pathway (Fig. 51).

9. Isoproterenol augmented cisplatin-induced apoptosis by HDAC8-dependent repression of TIPRL expression in H1299 cells

To study the biological effects of cAMP-induced increase in HDAC8 expression, we examined the effect of the HDAC8 increase on anticancer drug- or ionizing radiation-induced apoptosis. The activation of cAMP signaling with isoproterenol in cisplatin-treated or γ-ray irradiated H1299 cells increased the cleavage of caspase-3 and PARP, and annexin V-stained cell population, whereas HDAC8 knockdown using the HDAC8 shRNA abolished the apoptosis-augmenting effects of isoproterenol (Fig. 52-54), which indicates that cAMP signaling augments apoptosis in HDAC8-dependent manner. Next, to explore the underlying mechanism how HDAC8 augments cisplatin-induced apoptosis, we analyzed the effect of HDAC8 in

TOR signaling pathway regulator-like (TIPRL) expression. Human TIPRL, the mammalian ortholog of yeast TIP41 protein, was reported to inhibit the apoptosis induced by TRAIL [36], and its expression was found to be reduced via cAMP signaling (our unpublished data). Treatment with cisplatin increased the TIPRL protein levels, and exogenous HDAC8 expression decreased the cisplatin-induced TIPRL protein levels and increased the cisplatin-induced cleavage of caspase-3 and caspase-9 (Fig. 55). The knockdown of TIPRL with siRNA increased cleavage of caspase-3 and PARP in cisplatin-treated cells (Fig. 56), showing an anti-apoptotic role of TIPRL in H1299 cells. The isoproterenol treatment also decreased TIPRL expression in cisplatin-treated H1299 cells, and HDAC8 knockdown abolished the isoproterenol-induced decrease in TIPRL expression and augmentation of cleavage of caspase-3 and PARP (Fig. 57 and 58). To study the mechanism how HDAC8 decreases TIPRL expression, we analyzed the effect of HDAC8 of TIPRL mRNA levels. The isoproterenol treatment decreased TIPRL mRNA levels in cisplatin-treated H1299 cells, whereas the HDAC8 knockdown abolished the isoproterenol-induced decrease in mRNA levels (Fig. 59). To test whether the decrease in HDAC8 mRNA levels results from the decrease in TIPRL gene transcription, we analyzed the activity of a luciferase reporter that contains TIPRL promoter sequences. Treatment with cisplatin increased the activity of both the TIPRL reporter luciferases (TIPRL_R1-pLuc and TIPRL_R2-pLuc), and treatment with isoproterenol decreased the cisplatin-induced luciferase activity (Fig. 60). The HDAC8 knockdown abolished the effect of isoproterenol and restored the cisplatin-induced luciferase activity. To examine the effects of HDAC8-specific inhibitors on TIPRL expression, we treated the cell with PCI-34051 or NCC-149. The inhibitor treatments

did not abolish the isoproterenol effects on TIPRL expression and caspase-9 cleavage (Fig. 61 and 62). From these results, isoproterenol augments cisplatin-induced apoptosis by reducing the expression of TIPRL via the repression of transcription in HDAC8-dependent manner (Fig. 63).

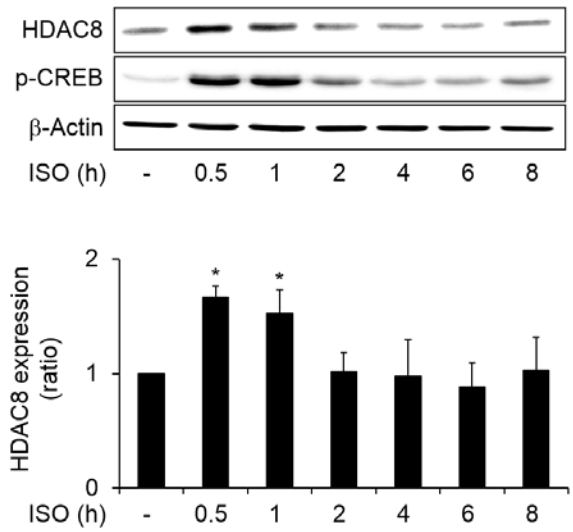

Figure 4. Time response of isoproterenol on HDAC8 expression

H1299 cells were treated with 20 μM isoproterenol (ISO) for various times (0-8 h), and the HDAC8 expression was analyzed by western blotting. The effect of isoproterenol on the phosphorylation of CREB was confirmed by western blot analysis using a specific antibody against phosphorylated CREB (S133). Asterisks (*) on the bar graph indicate a statistically significant difference compared with the corresponding control (*$p < 0.05$, Mann-Whitney U test).

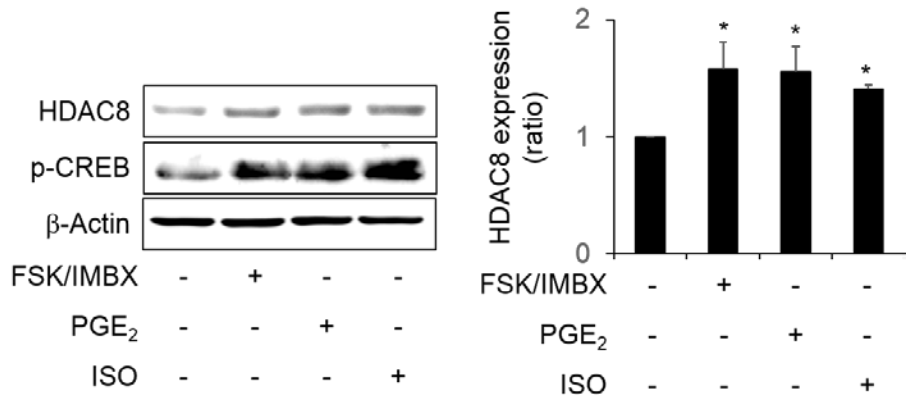

Figure 5. Effect of forskolin/IMBX, PGE2 or isoproterenol on HDAC8 expression

H1299 cells were treated with 20 μM forskolin (FSK)/100 μM IBMX, 20 μM PGE2, or 20 μM isoproterenol (ISO) for 30 min and a subsequent western blot analysis. Asterisks (*) on the bar graph indicate a significant difference compared with the respective control cells (*$p < 0.05$, Mann-Whitney U test).

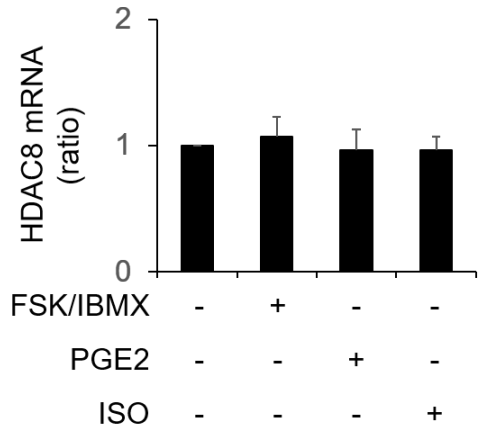

Figure 6. Effect of forskolin/IBMX, PGE2 or isoproterenol on HDAC8 mRNA levels

H1299 cells were treated with 20 μM forskolin (FSK)/100 μM IBMX, 20 μM PGE2, or 20 μM isoproterenol (ISO) for 30 min. HDAC8 mRNA levels were analyzed by qRT-PCR. The amounts of HDAC8 mRNA were normalized to the levels of GAPDH, and the results are presented as a ratio to the values of the untreated control.

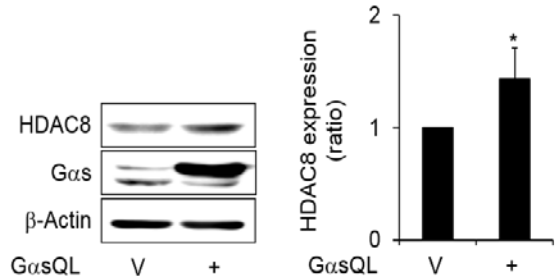

Figure 7. Effect of GαsQL on HDAC8 expression in A549 cells

A549 cells were transfected with the pcDNA3.1(+) vector (V) or GαsQL by lipofectamine for 24 h, and a subsequent western blot analysis. The asterisk (*) on the bar graph indicates a statistically significant difference compared with the corresponding control (*$p < 0.05$, Mann-Whitney U test).

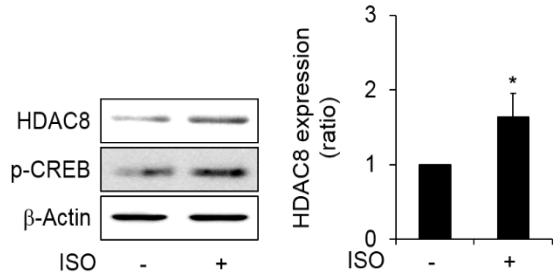

Figure 8. Effect of isoproterenol on HDAC8 expression in A549 cells

A549 cells were treated with 20 μM isoproterenol (ISO) for 30 min, and a subsequent western blot analysis. The asterisk (*) on the bar graph indicates a statistically significant difference compared with the corresponding control (*$p < 0.05$, Mann-Whitney U test).

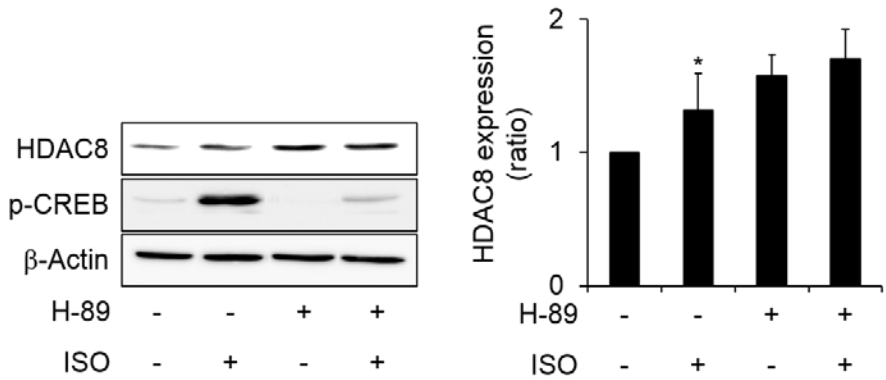

Figure 9. Effect of H-89 on isoproterenol-induced HDAC8 expression

H1299 cells were pretreated with 20 μM H-89 for 1 h, followed by the 20 μM isoproterenol (ISO) for 30 min, and a subsequent western blot analysis. The asterisk (*) on the bar graph indicates a statistically significant difference compared with the corresponding control (*$p < 0.05$, Mann-Whitney U test).

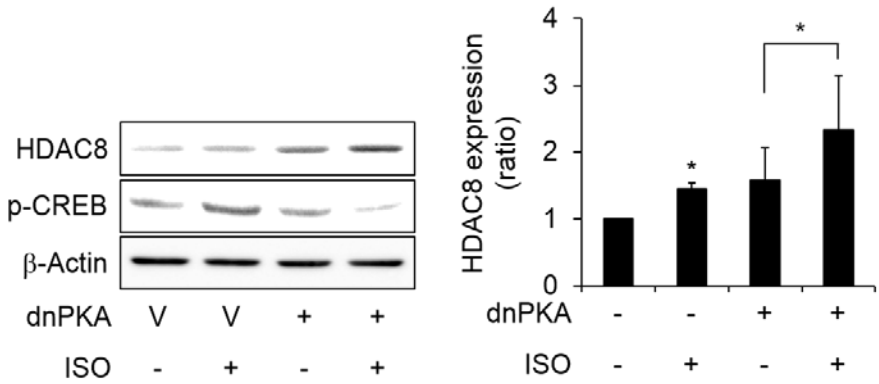

Figure 10. Effect of dominant-negative PKA on isoproterenol-induced HDAC8 expression

For transient expression, H1299 cells were transfected with a vector (V) or dnPKA by lipofectamine for 48 h. Before harvesting, the cells were treated with 20 μM isoproterenol (ISO) for 30 min, and a subsequent western blot analysis. Asterisks (*) on the bar graph indicate a statistically significant difference compared with the corresponding control (*$p < 0.05$, Mann-Whitney U test).

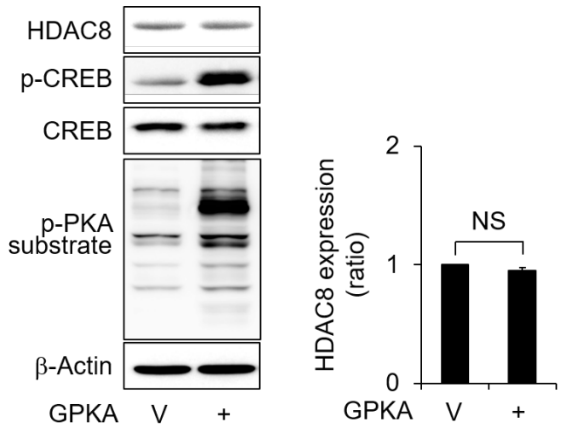

Figure 11. Effect of GPKA on HDAC8 expression

H1299 cells were transfected with a vector (V) or GPKA (constitutively active PKA) by lipofectamine for 24 h, and a subsequent western blot analysis. NS indicates no statistically significant difference compared with the corresponding control (*p < 0.05, Mann-Whitney U test).

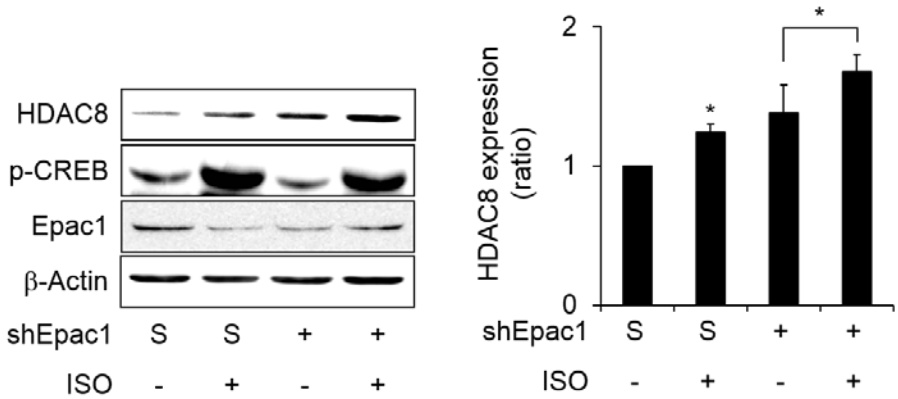

Figure 12. Effect of shEpac1 on isoproterenol-induced HDAC8 expression

For transient expression, H1299 cells were transfected with a scramble shRNA (S) or shEpac1 #1 by calcium phosphate transfection for 24 h. Before harvesting, the cells were treated with 20 μM isoproterenol (ISO) for 30 min, and a subsequent western blot analysis. Asterisks (*) on the bar graph indicate a statistically significant difference compared with the corresponding control (*$p < 0.05$, Mann-Whitney U test).

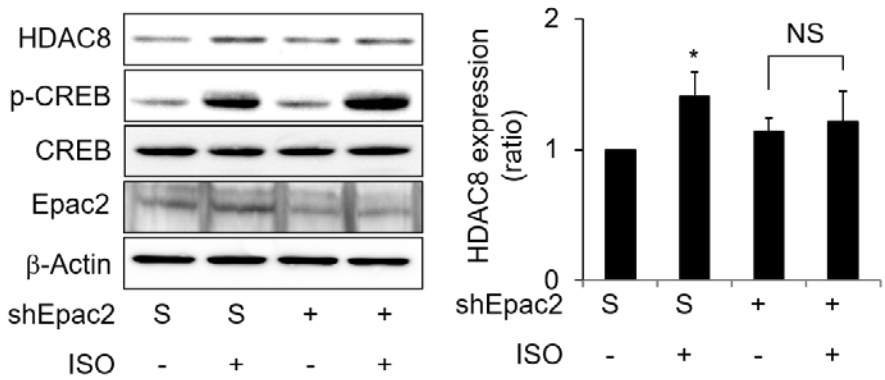

Figure 13. Effect of shEpac2 on isoproterenol-induced HDAC8 expression

For transient expression, H1299 cells were transfected with a scrambled shRNA (S) or shEpac2 #5 by lipofectamine for 48 h. Before harvesting, the cells were treated with 20 μM isoproterenol (ISO) for 30 min, and a subsequent western blot analysis. The asterisk (*) on the bar graph indicates a statistically significant difference compared with the corresponding control, and NS indicates no statistically significant difference compared with the corresponding control (*$p < 0.05$, Mann-Whitney U test).

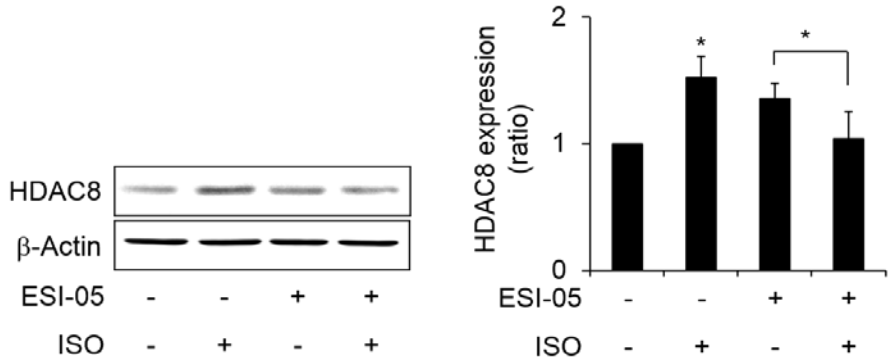

Figure 14. Effect of ESI-05 on isoproterenol-induced HDAC8 expression

H1299 cells, which have been pretreated with or without 10 μM ESI-05 (Epac2-selective inhibitor) for 30 min, were treated with 20 μM isoproterenol (ISO) for 30 min and a subsequent western blot analysis. Asterisks (*) on the bar graph indicate a statistically significant difference compared with the corresponding control (*p < 0.05, Mann-Whitney U test).

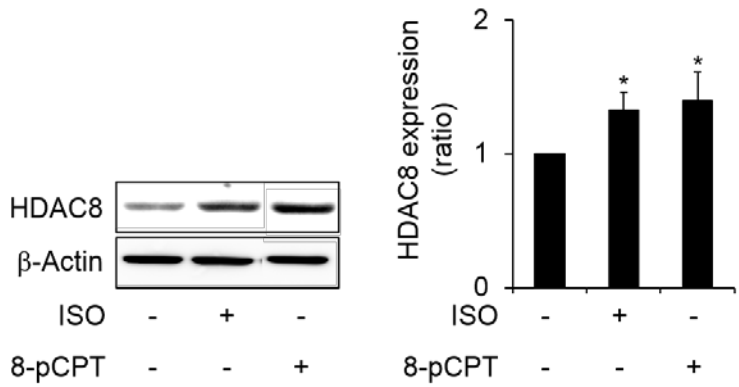

Figure 15. Effect of 8-pCPT-cAMP on HDAC8 expression

H1299 cells were incubated with 20 μM isoproterenol (ISO) or 20 μM 8-pCPT-cAMP (Epac-selective agonist) for 30 min, and a subsequent western blot analysis. Asterisks (*) on the bar graph indicate a statistically significant difference compared with the corresponding control (*$p < 0.05$, Mann-Whitney U test).

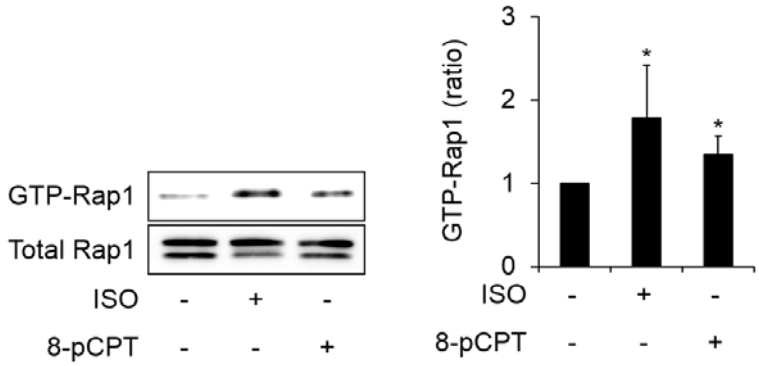

Figure 16. Effect of isoproterenol or 8-pCPT-cAMP on GTP-bound Rap1

H1299 cells were incubated with 20 μM isoproterenol (ISO) or 20 μM 8-pCPT-cAMP for 30 min. A Rap1 activation assay was performed on the cell lysates. Cell lysates were precipitated with GST-RalGDS(RBD), and precipitated proteins were analyzed by anti-Rap1 western blotting. Asterisks (*) on the bar graph indicate a statistically significant difference compared with the corresponding control (*$p < 0.05$, Mann-Whitney U test).

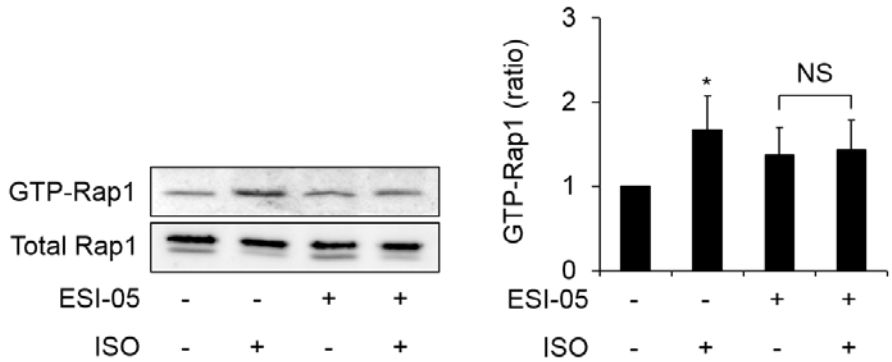

Figure 17. Effect of ESI-05 on isoproterenol-induced GTP-bound Rap1

H1299 cells, which have been pretreated with or without 10 μM ESI-05 for 30 min, were treated with 20 μM isoproterenol (ISO) for 30 min before pull down assay. The asterisk (*) on the bar graph indicates a statistically significant difference compared with the corresponding control and NS indicates no statistically significant difference compared with the corresponding control (*$p < 0.05$, Mann-Whitney U test).

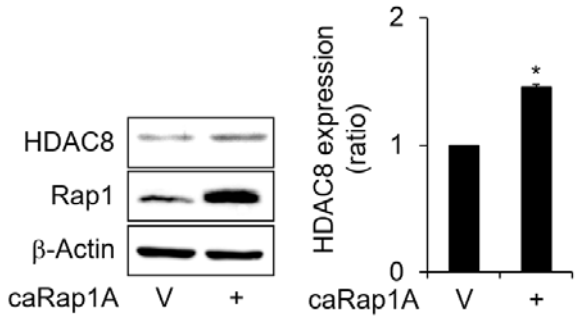

Figure 18. Effect of constitutively active Rap1A (V12) on HDAC8 expression

For transient expression, H1299 cells were transfected with a vector (V) or caRap1A (V12) by lipofectamine for 24 h, and a subsequent western blot analysis. The asterisk (*) on the bar graph indicates a statistically significant difference compared with the corresponding control (*$p < 0.05$, Mann-Whitney U test).

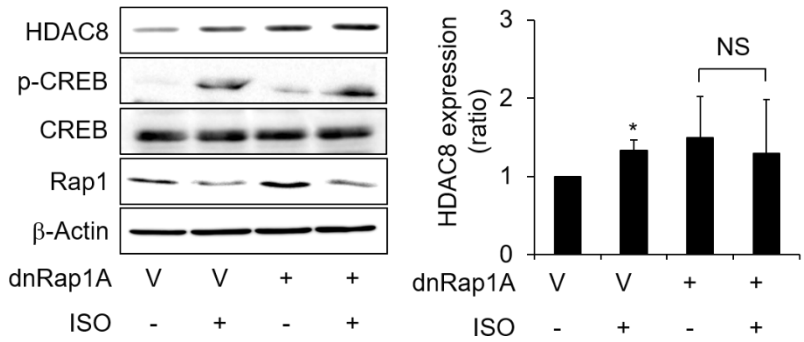

Figure 19. Effect of dominant-negative Rap1A (N17) on isoproterenol-induced HDAC8 expression

For transient expression, H1299 cells were transfected with a vector (V) or dnRap1A (N17) by lipofectamine for 48 h. Before harvesting, the cells were treated with 20 μM isoproterenol (ISO) for 30 min, and a subsequent western blot analysis. The asterisk (*) on the bar graph indicates a statistically significant difference compared with the corresponding control and NS indicates no statistically significant difference compared with the corresponding control (*$p < 0.05$, Mann-Whitney U test).

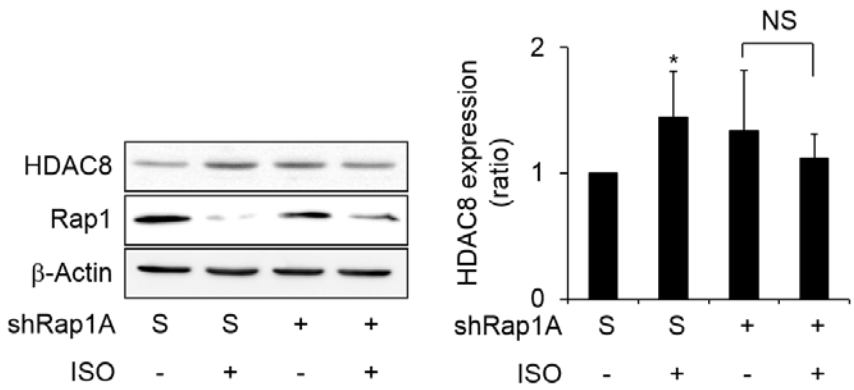

Figure 20. Effect of shRap1A on isoproterenol-induced HDAC8 expression

For transient expression, H1299 cells were transfected with a scrambled shRNA (S) or shRap1A #2 by lipofectamine for 48 h. Before harvesting, the cells were treated with 20 μM isoproterenol (ISO) for 30 min, and a subsequent western blot analysis. The asterisk (*) on the bar graph indicates a statistically significant difference compared with the corresponding control and NS indicates no statistically significant difference compared with the corresponding control (*$p < 0.05$, Mann-Whitney U test).

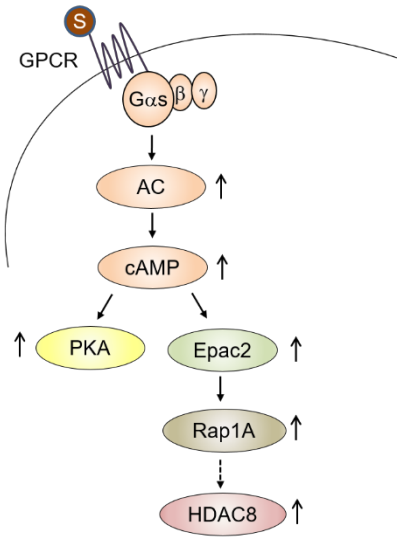

Figure 21. A suggested model for cAMP signaling system increases HDAC8 expression via Epac2-Rap1A pathway in NSCLC cells

The solid lines indicate proven signaling pathways, and the dotted line indicates suggested signaling pathways**.**

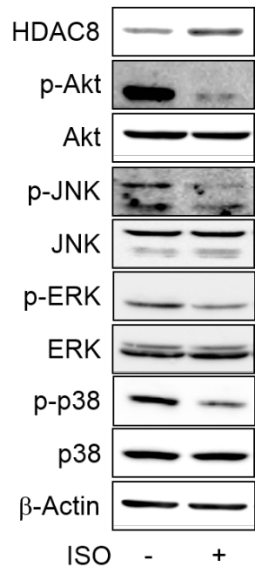

Figure 22. Effect of isoproterenol on the phosphorylation of Akt and MAPK proteins

H1299 cells were incubated with 20 μM isoproterenol (ISO) for 30 min, and a subsequent western blot analysis.

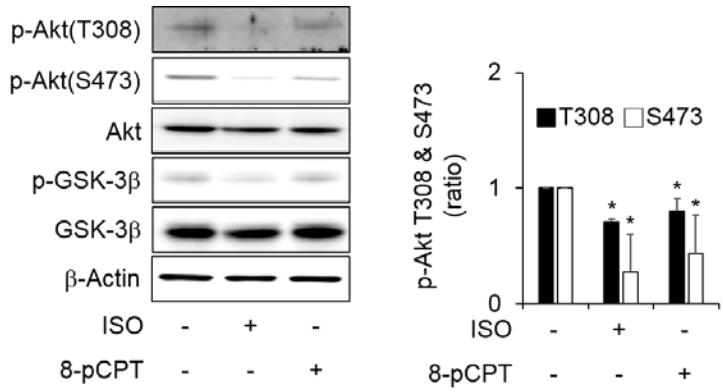

Figure 23. Effect of isoproterenol or 8-pCPT-cAMP on Akt phosphorylation

H1299 cells were treated with 20 μM isoproterenol (ISO) or 20 μM 8-pCPT-cAMP for 30 min, and a subsequent western blot analysis (black bar: p-Akt T308, white bar: p-Akt S473). Asterisks (*) on the bar graph indicate a statistically significant difference compared with the corresponding control (*$p < 0.05$, Mann-Whitney U test).

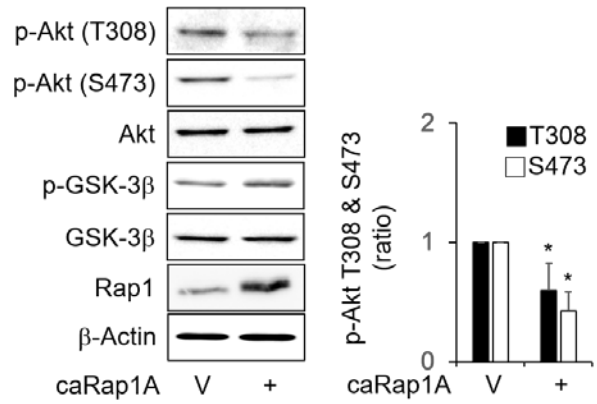

Figure 24. Effect of constitutively active Rap1A (V12) on Akt phosphorylation

For transient expression, H1299 cells were transfected with a vector (V) or caRap1A (V12) by lipofectamine for 24 h, and a subsequent western blot analysis (black bar: p-Akt T308, white bar: p-Akt S473). Asterisks (*) on the bar graph indicate a statistically significant difference compared with the corresponding control (*p < 0.05, Mann-Whitney U test).

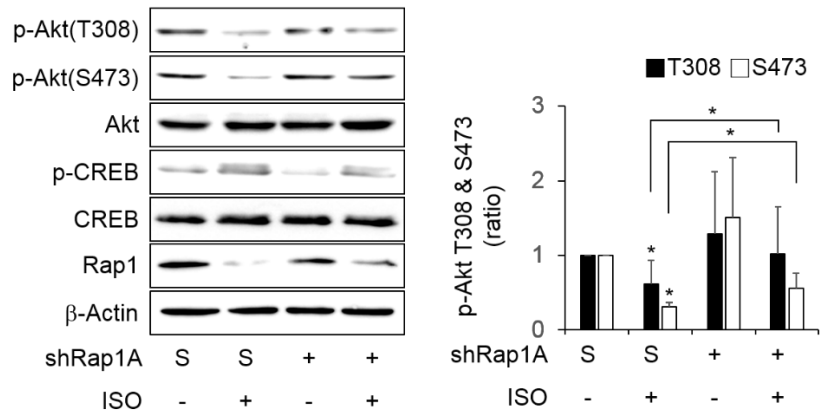

Figure 25. Effect of shRap1A on isoproterenol-decreased Akt phosphorylation

For transient expression, H1299 cells were transfected with a scrambled shRNA (S) or shRap1A #2 by lipofectamine for 48 h. Before harvesting, the cells were treated with 20 μM isoproterenol (ISO) for 30 min, and a subsequent western blot analysis (black bar: p-Akt T308, white bar: p-Akt S473). Asterisks (*) on the bar graph indicate a statistically significant difference compared with the corresponding control (*$p < 0.05$, Mann-Whitney U test).

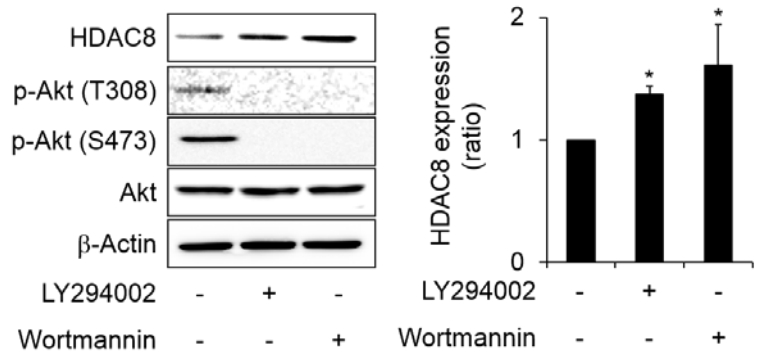

Figure 26. Effect of LY294002 or wortmannin on HDAC8 expression

H1299 cells were incubated with PI3K inhibitors (10 μM LY294002 or 100 nM wortmannin) for 30 min, and a subsequent western blot analysis. Asterisks (*) on the bar graph indicate a statistically significant difference compared with the corresponding control (*$p < 0.05$, Mann-Whitney U test).

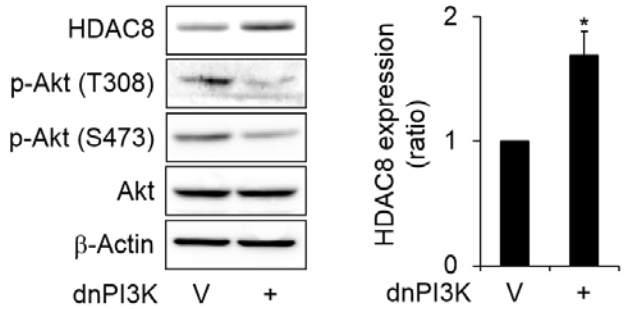

Figure 27. Effect of dominant-negative PI3K on HDAC8 expression

For transient expression, H1299 cells were transfected with a vector (V) or dnPI3K (⊿p85 PI3K) by lipofectamine for 24 h, and a subsequent western blot analysis. The asterisk (*) on the bar graph indicates a statistically significant difference compared with the corresponding control (*$p < 0.05$, Mann-Whitney U test).

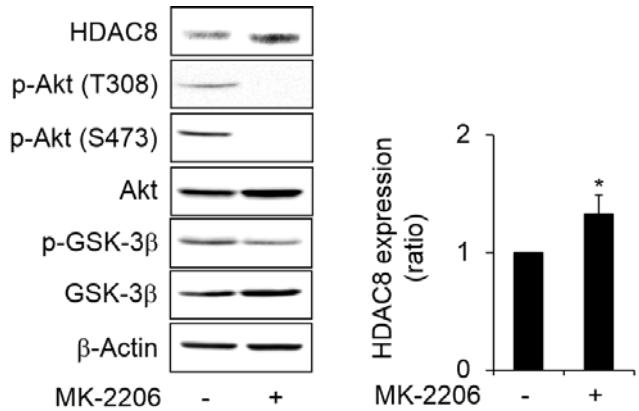

Figure 28. Effect of MK-2206 on HDAC8 expression

H1299 cells were treated with 10 μM MK-2206 (Akt inhibitor) for 30 min, and a subsequent western blot analysis. The asterisk (*) on the bar graph indicates a statistically significant difference compared with the corresponding control (*p < 0.05, Mann-Whitney U test).

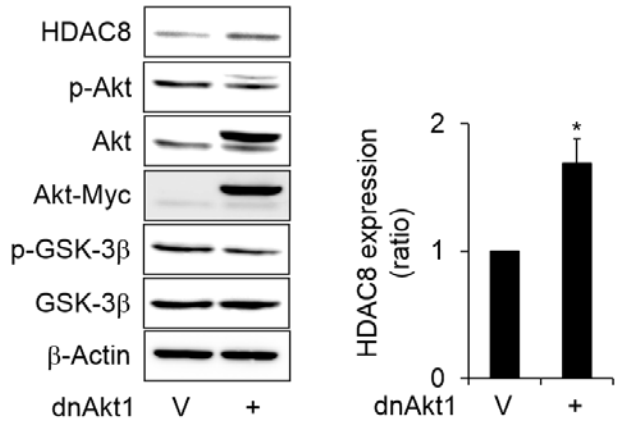

Figure 29. Effect of dominant-negative Akt1 on HDAC8 expression

For transient expression, H1299 cells were transfected with the pUSE vector (V) or Myc-DN-Akt1 (dnAkt1) by lipofectamine for 24 h, and a subsequent western blot analysis. The asterisk (*) on the bar graph indicates a statistically significant difference compared with the corresponding control (*$p < 0.05$, Mann-Whitney U test).

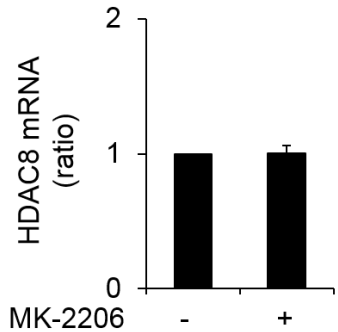

Figure 30. Effect of MK-2206 on HDAC8 mRNA levels

H1299 cells were treated with 10 μM MK-2206 (Akt inhibitor) for 30 min. HDAC8 mRNA levels were analyzed by qRT-PCR. The amounts of HDAC8 mRNA were normalized to the levels of GAPDH, and the results are presented as a ratio to the values of the untreated control.

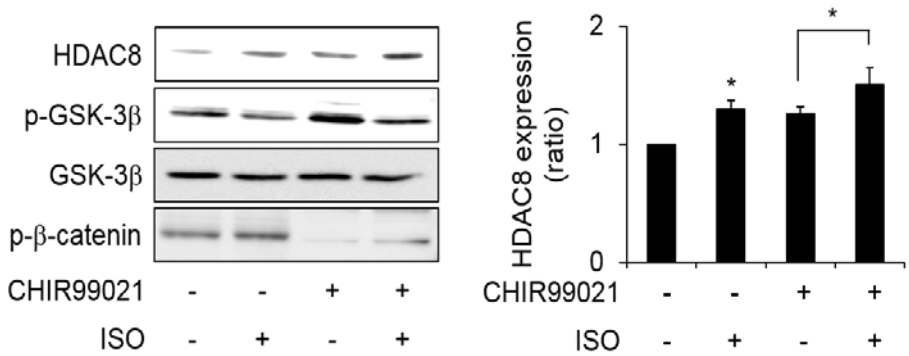

Figure 31. Effect of CHIR99021 on isoproterenol-induced HDAC8 expression

H1299 cells were pretreated with 10 μM CHIR99021 (GSK-3β inhibitor) for 30 min, followed by the 20 μM isoproterenol (ISO) treatment for 30 min, and a subsequent western blot analysis. Asterisks (*) on the bar graph indicate a statistically significant difference compared with the corresponding control (*$p < 0.05$, Mann-Whitney U test).

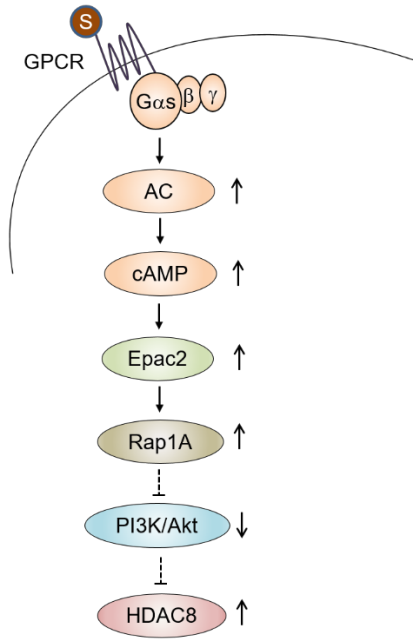

Figure 32. A suggested model for cAMP signaling system increases HDAC8 expression via Epac2-Rap1A-mediated inhibition of PI3K/Akt pathways in NSCLC cells

The solid lines indicate proven signaling pathways, and the dotted lines indicate suggested signaling pathways**.**

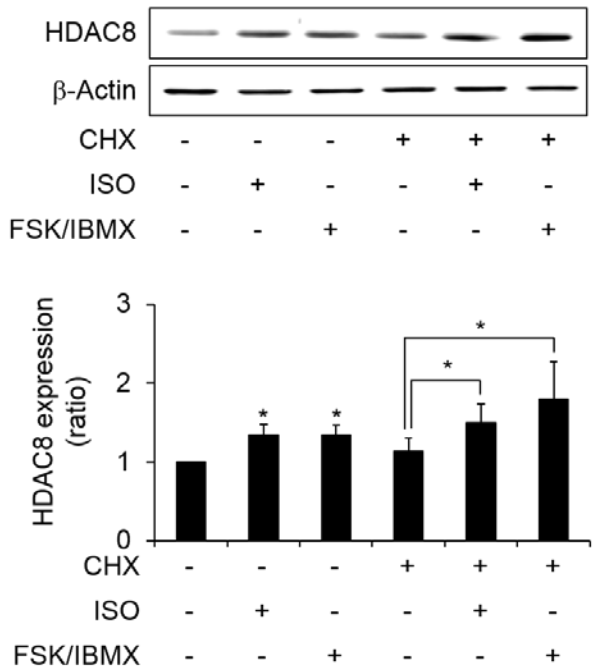

Figure 33. Effect of cycloheximide on the isoproterenol- or forskolin/IBMX-induced HDAC8 expression

H1299 cells, which had been pretreated with 50 μg/ml cycloheximide (CHX) for 30 min, were treated with 20 μM isoproterenol (ISO) or 20 μM forskolin (FSK)/100 μM IBMX, and a subsequent western blot analysis. Asterisks (*) on the bar graph indicate a statistically significant difference compared with the corresponding control (*$p < 0.05$, Mann-Whitney U test).

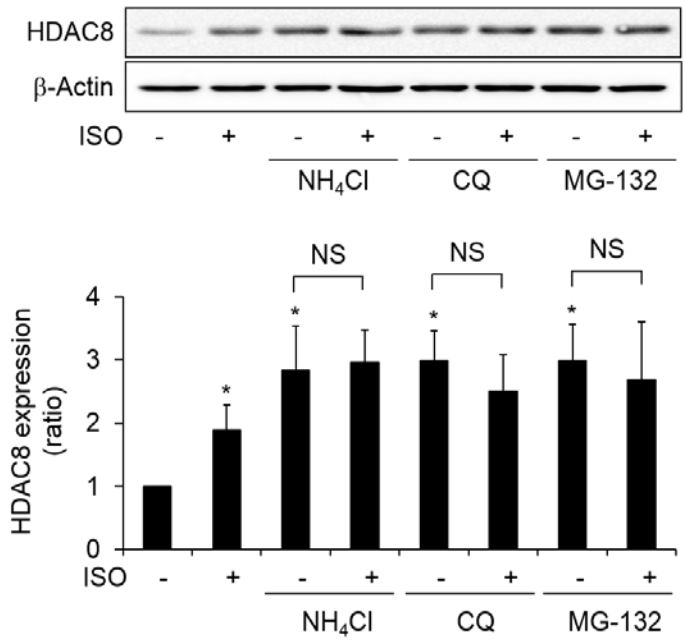

Figure 34. Effect of lysosomal or proteasomal degradation on isoproterenol-induced HDAC8 expression

H1299 cells were pretreated with 10 mM NH_4Cl, 20 μM chloroquine (CQ), or 10 μM MG-132 for 4 h prior to 20 μM isoproterenol (ISO) treatment for 30 min, and a subsequent western blot analysis. Asterisks (*) on the bar graph indicate a statistically significant difference compared with the corresponding control and NS indicates no statistically significant difference compared with the corresponding control (*$p < 0.05$, Mann-Whitney U test).

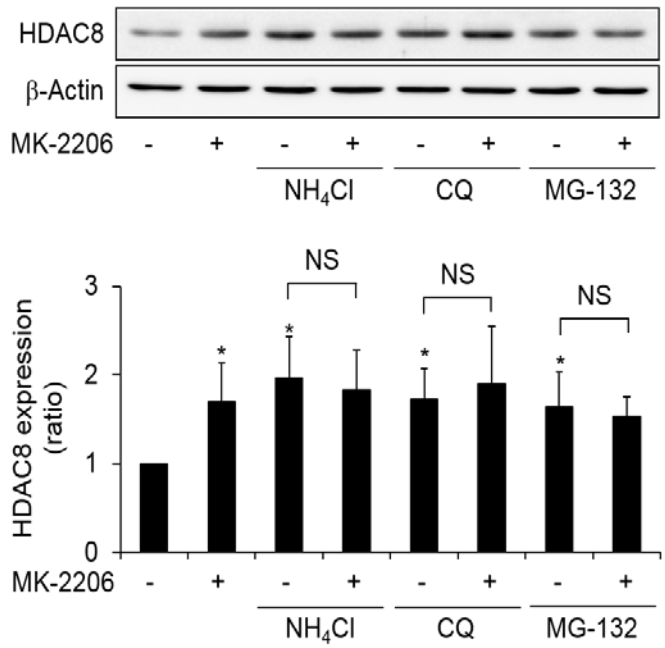

Figure 35. Effect of lysosomal or proteasomal degradation on MK-2206-induced HDAC8 expression

H1299 cells were pretreated with 10 mM NH_4Cl, 20 μM chloroquine (CQ), or 10 μM MG-132 for 4 h prior to 10 μM MK-2206 treatment for 30 min, and a subsequent western blot analysis. Asterisks (*) on the bar graph indicate a statistically significant difference compared with the corresponding control and NS indicates no statistically significant difference compared with the corresponding control (*$p < 0.05$, Mann-Whitney U test).

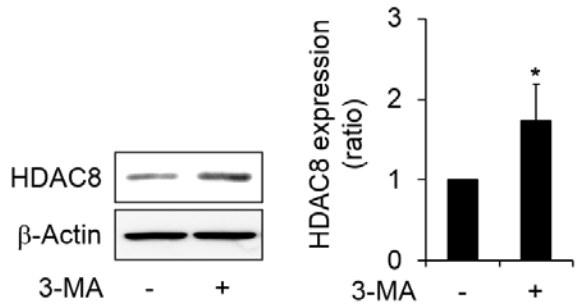

Figure 36. Effect of 3-methyladenine on HDAC8 expression

H1299 cells were treated with 10 mM 3-methyladenine (3-MA, autophagy inhibitor) for 30 min, and a subsequent western blot analysis. The asterisk (*) on the bar graph indicates a statistically significant difference compared with the corresponding control (*$p < 0.05$, Mann-Whitney U test).

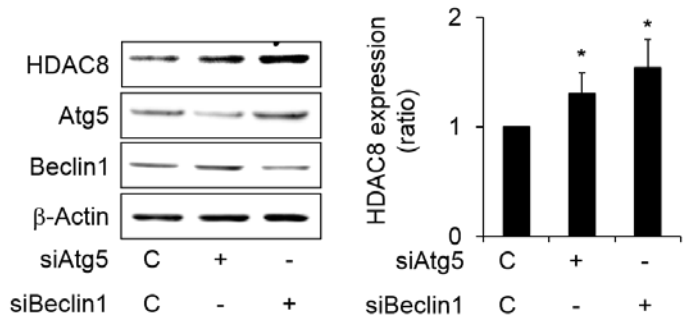

Figure 37. Effect of siAtg5 or siBeclin1 on HDAC8 expression

For transient expression, H1299 cells were transfected with the control siRNA (C) or siAtg5/siBeclin1 by lipofectamine for 48 h, and a subsequent western blot analysis. Asterisks (*) on the bar graph indicate a statistically significant difference compared with the corresponding control (*$p < 0.05$, Mann-Whitney U test).

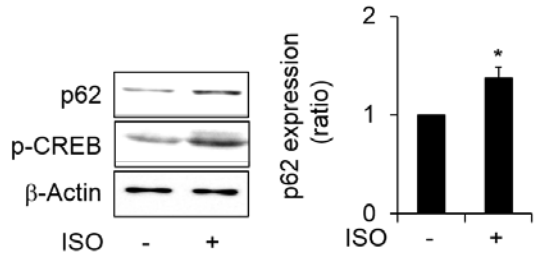

Figure 38. Effect of isoproterenol on p62 expression

H1299 cells were treated with 20 μM isoproterenol (ISO) for 30 min, and a subsequent western blot analysis. The asterisk (*) on the bar graph indicates a statistically significant difference compared with the corresponding control (*p < 0.05, Mann-Whitney U test).

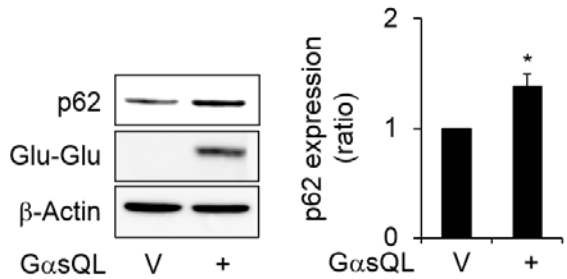

Figure 39. Effect of GαsQL on p62 expression

H1299 cells were transfected with the pcDNA3.1(+) vector (V) or GαsQL and then incubated for 24 h and a subsequent western blot analysis. The asterisk (*) on the bar graph indicates a statistically significant difference compared with the corresponding control (*$p < 0.05$, Mann-Whitney U test).

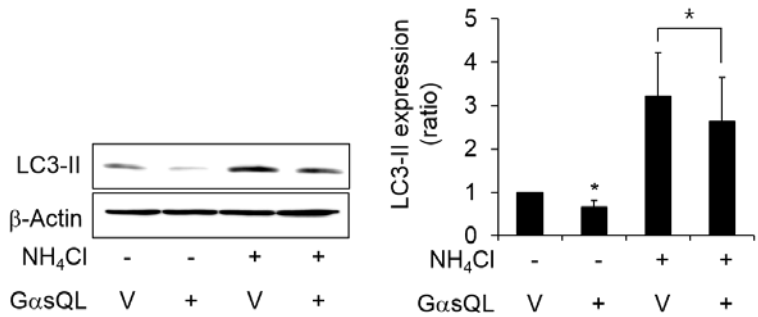

Figure 40. Effect of GαsQL on LC3-II expression

H1299 cells were transfected with the pcDNA3.1(+) vector (V) or GαsQL and then incubated for 24 h prior to treatment with 10 mM NH_4Cl for 4 h, and a subsequent western blot analysis. Asterisks (*) on the bar graph indicate a statistically significant difference compared with the corresponding control (*$p < 0.05$, Mann-Whitney U test).

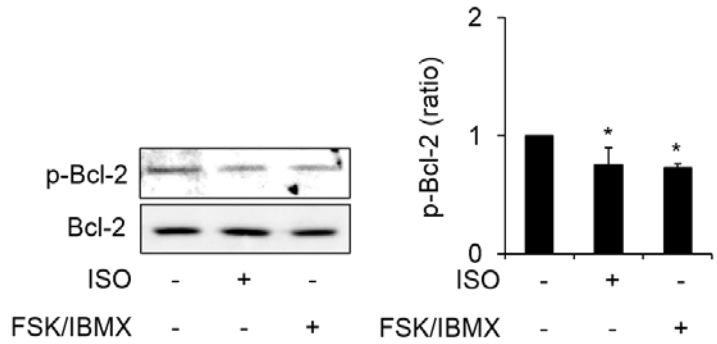

Figure 41. Effect of isoproterenol or forskolin/IBMX on Bcl-2 phosphorylation

H1299 cells were treated with 20 μM isoproterenol (ISO) or 20 μM forskolin (FSK)/100 μM IBMX for 30 min, and a subsequent western blot analysis. Asterisks (*) on the bar graph indicate a statistically significant difference compared with the corresponding control (*$p < 0.05$, Mann-Whitney U test).

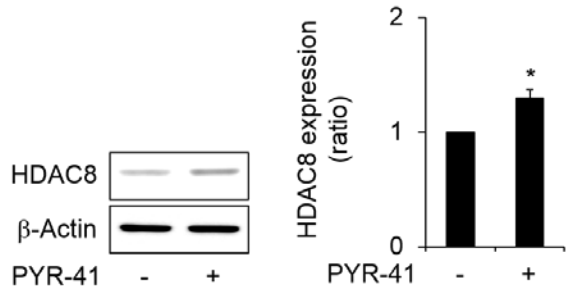

Figure 42. Effect of PYR-41 on HDAC8 expression

H1299 cells treatment with 10 μM PYR-41 (E1 ubiquitin inhibitor) for 4 h, and a subsequent western blot analysis. The asterisk (*) on the bar graph indicates a statistically significant difference compared with the corresponding control (*p < 0.05, Mann-Whitney U test).

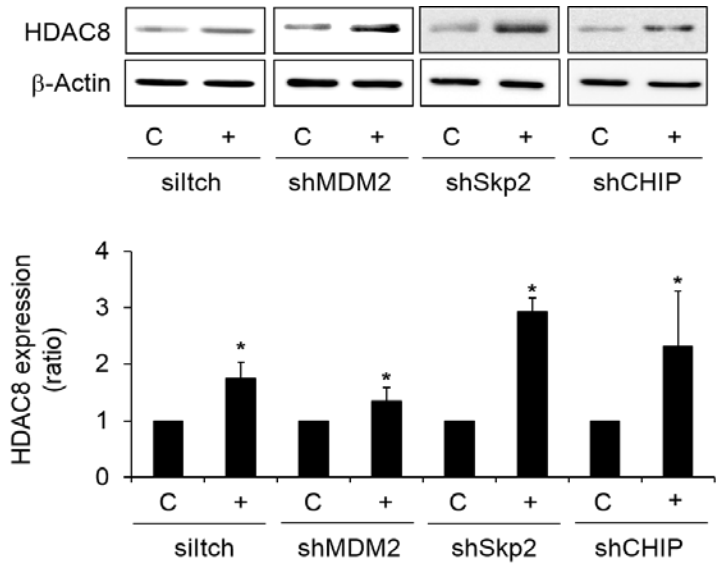

Figure 43. Effects of E3 ligases on HDAC8 expression

For transient expression, H1299 cells were transfected with a scrambled shRNA /control siRNA (C) or siItch, shMDM2, shSkp2, or shCHIP by lipofectamine for 48 h, and a subsequent western blot analysis. Asterisks (*) on the bar graph indicate a statistically significant difference compared with the corresponding control (*p < 0.05, Mann-Whitney U test).

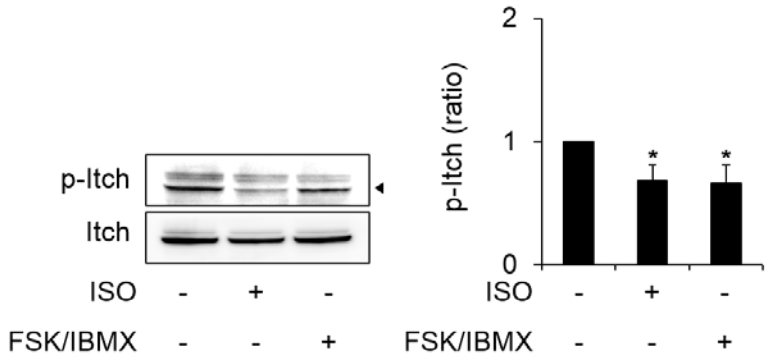

Figure 44. Effect of isoproterenol or forskolin/IBMX on Itch phosphorylation

H1299 cells were treated with 20 μM isoproterenol (ISO) or 20 μM forskolin (FSK)/100 μM IBMX for 30 min, and a subsequent western blot analysis. Asterisks (*) on the bar graph indicate a statistically significant difference compared with the corresponding control (*$p < 0.05$, Mann-Whitney U test).

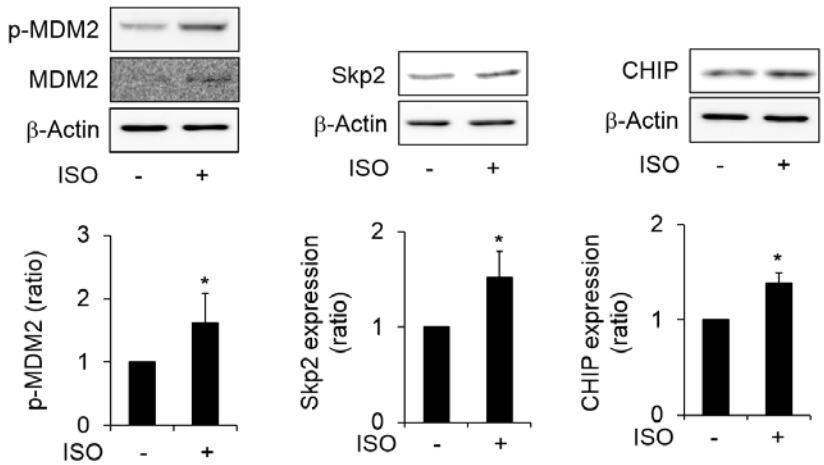

Figure 45. Effect of isoproterenol on E3 ligases expression and MDM2 phosphorylation

H1299 cells were treated with 20 μM isoproterenol (ISO) for 30 min and a subsequent western blot analysis. Asterisks (*) on the bar graphs indicate a statistically significant difference compared with the corresponding control (*$p < 0.05$, Mann-Whitney U test).

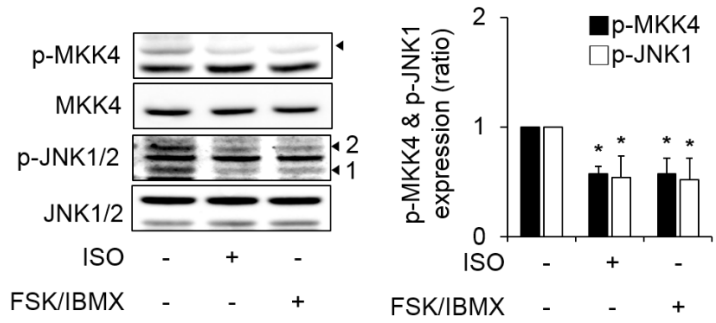

Figure 46. Effect of isoproterenol or forskolin/IBMX on the phosphorylation of JNK1 and MKK4

H1299 cells were treated with 20 μM isoproterenol (ISO) or 20 μM forskolin (FSK)/100 μM IBMX for 30 min, and a subsequent western blot analysis (black bar: p-MKK4, white bar: p-JNK1). Asterisks (*) on the bar graph indicate a statistically significant difference compared with the corresponding control (*$p < 0.05$, Mann-Whitney U test).

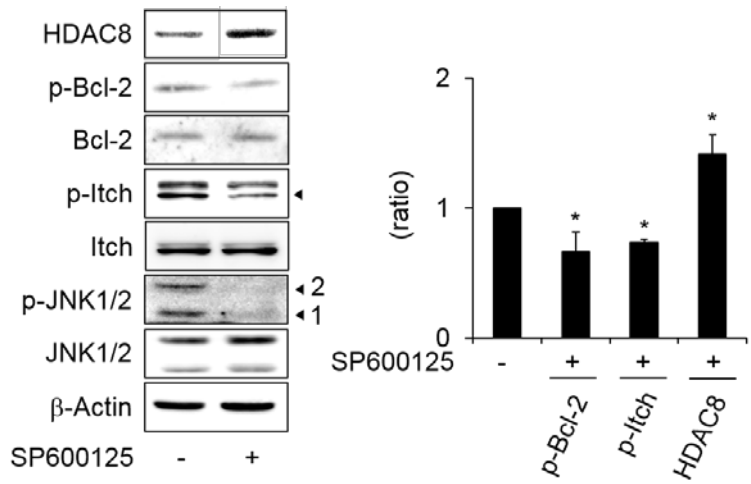

Figure 47. Effect of SP600125 on the phosphorylation of Bcl-2 and Itch

H1299 cells were treated with 10 μM SP600125 (JNK inhibitor) for 30 min, and a subsequent western blot analysis. Asterisks (*) on the bar graph indicate a statistically significant difference compared with the corresponding control (*p < 0.05, Mann-Whitney U test).

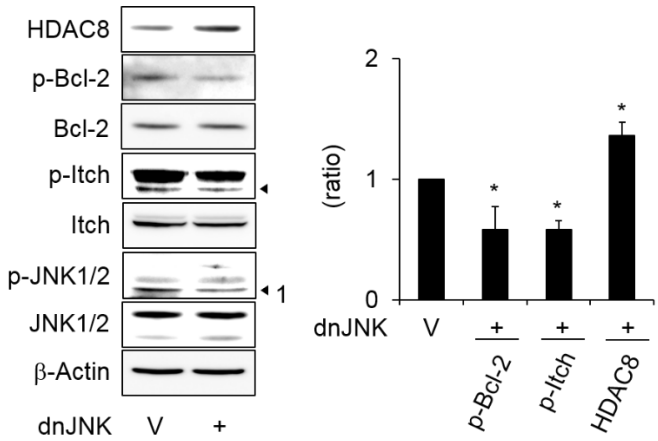

Figure 48. Effect of dominant-negative JNK on the phosphorylation of Bcl-2 and Itch

For transient expression, H1299 cells were transfected with the pcDNA3 vector (V) or dnJNK by lipofectamine for 48 h, and a subsequent western blot analysis. Asterisks (*) on the bar graph indicate a statistically significant difference compared with the corresponding control (*$p < 0.05$, Mann-Whitney U test).

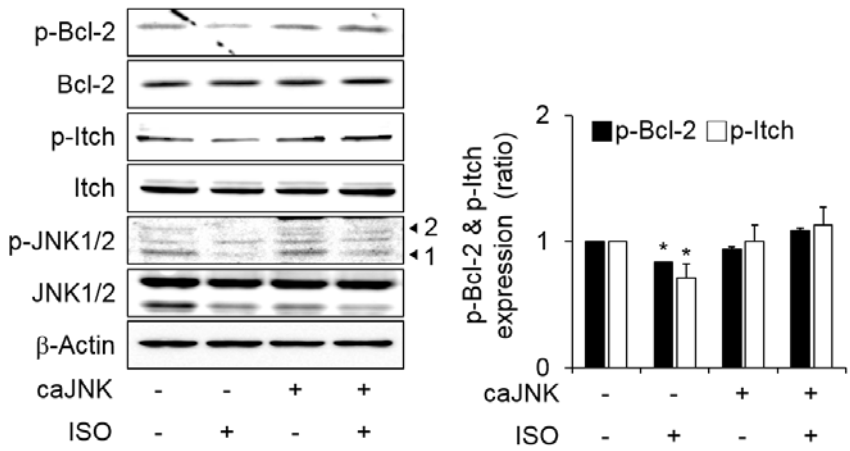

Figure 49. Effect of constitutively active JNK on isoproterenol-decreased phosphorylation of Bcl-2 and Itch

For transient expression, H1299 cells were transfected with a vector (V) or caJNK by lipofectamine for 48 h. Before harvesting, the cells were treated with 20 μM isoproterenol (ISO) for 30 min, and a subsequent western blot analysis (black bar: p-Bcl2, white bar: p-Itch). Asterisks (*) on the bar graph indicate a statistically significant difference compared with the corresponding control (*$p < 0.05$, Mann-Whitney U test).

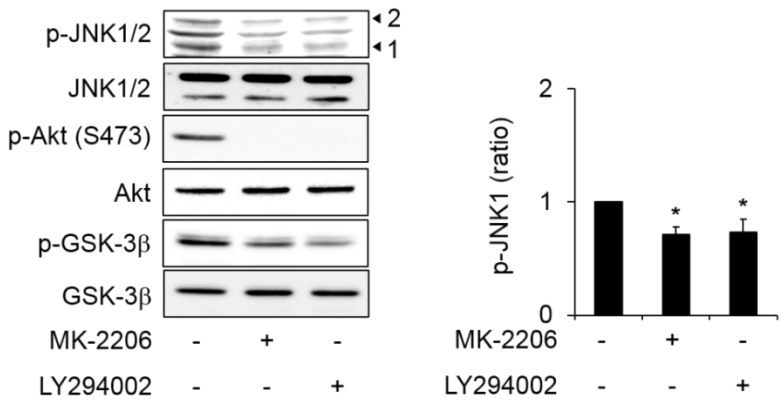

Figure 50. Effect of MK-2206 or LY294002 on JNK phosphorylation

H1299 cells were treated with 10 μM MK-2206 or 10 μM LY294002 for 30 min, and a subsequent western blot analysis. Asterisks (*) on the bar graph indicate a statistically significant difference compared with the corresponding control (*p < 0.05, Mann-Whitney U test).

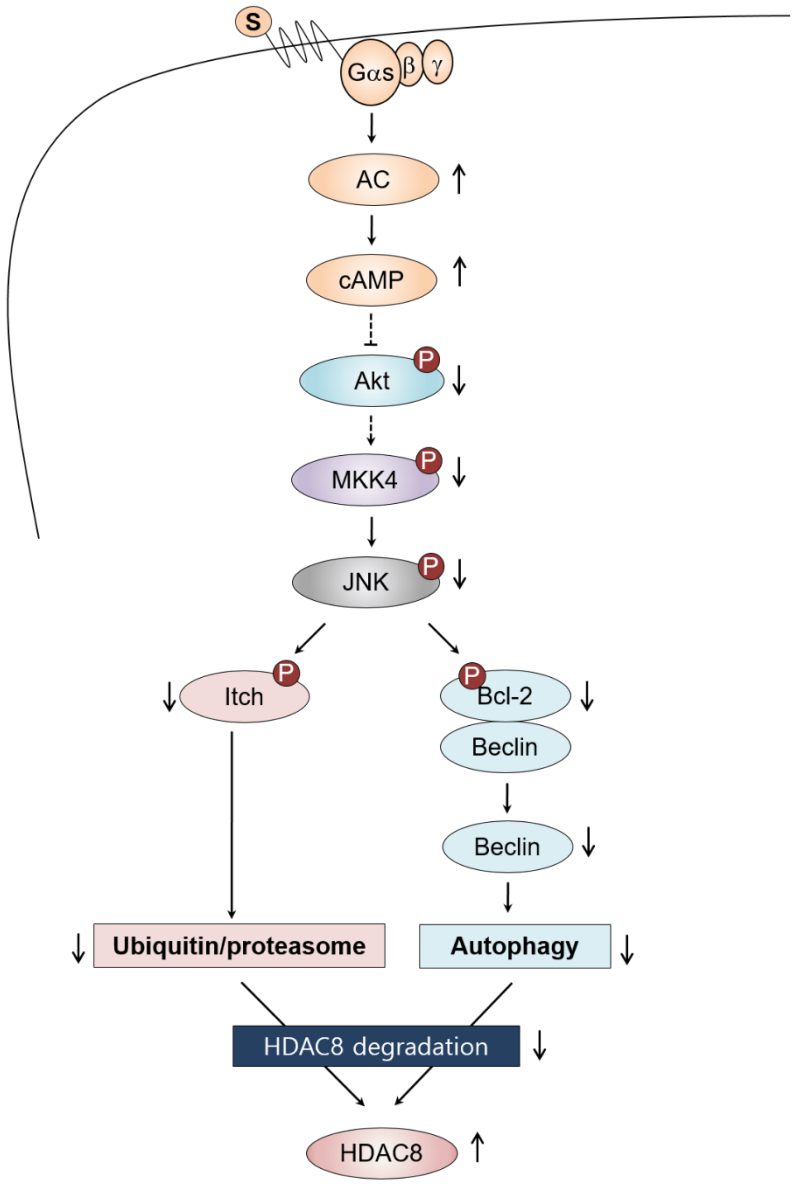

Figure 51. A suggested model for how cAMP signaling system increases HDAC8 protein levels by inhibition autophagy and the ubiquitin-proteasome system in H1299 cells

The solid lines indicate proven signaling pathways, and the dotted lines indicate suggested signaling pathways**.**

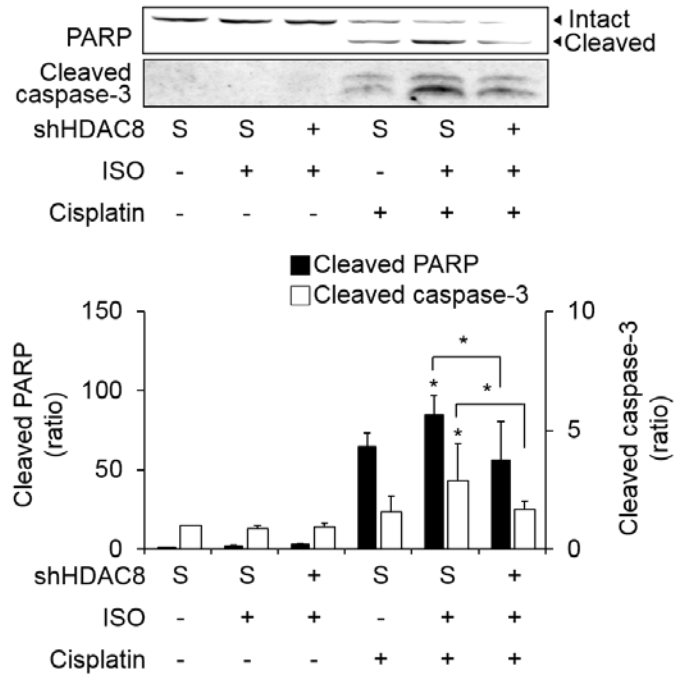

Figure 52. Effects of isoproterenol and HDAC8 on cisplatin-induced cleavage of PARP and caspase-3

For transient expression, H1299 cells were transfected with a scrambled shRNA (S) or shHDAC8 #3 by lipofectamine for 24 h, and then cells were treated with 20 μM isoproterenol (ISO) for 30 min prior to 50 μM cisplatin treatment for 48 h, and a subsequent western blot analysis (black bar: cleaved PARP, white bar: cleaved caspase-3). Asterisks (*) on the bar graph indicate a statistically significant difference compared with the corresponding control (*$p < 0.05$, Mann-Whitney U test).

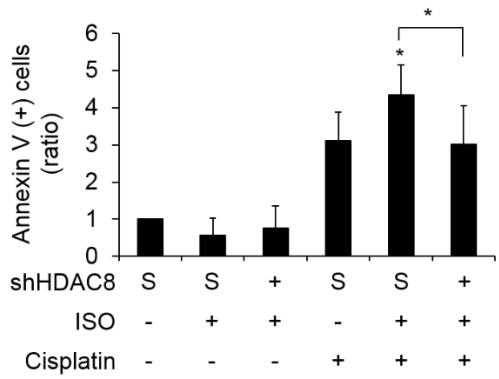

Figure 53. Effects of isoproterenol and HDAC8 on cisplatin-induced annexin V-staining of H1299 cells

For transient expression, H1299 cells were transfected with a scrambled shRNA (S) or shHDAC8 #3 by lipofectamine for 24 h, and then cells were treated with 20 μM isoproterenol (ISO) for 30 min prior to 50 μM cisplatin treatment for 48 h. Flow cytometric analysis of apoptosis was performed using FITC annexin V apoptosis detection kit I and FACSCanto II flow cytometer. Asterisks (*) on the bar graph indicate a statistically significant difference compared with the corresponding control (*$p < 0.05$, Mann-Whitney U test).

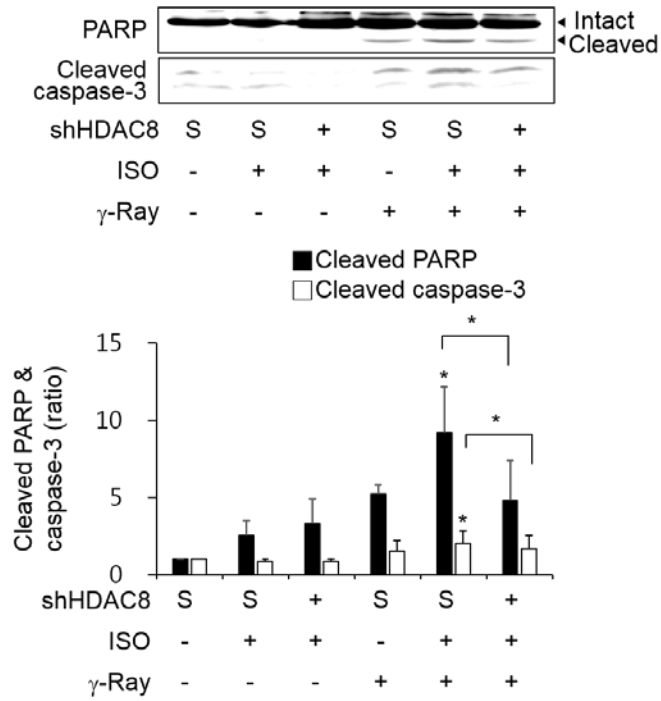

Figure 54. Effects of isoproterenol and HDAC8 on γ-ray-induced cleavage of PARP and caspase-3

For transient expression, H1299 cells were transfected with a scrambled shRNA (S) or shHDAC8 #3 by lipofectamine for 24 h, and then cells were treated with 20 μM isoproterenol (ISO) for 30 min before irradiation with γ-rays (10 Gy) for 24, and a subsequent western blot analysis (black bar: cleaved PARP, white bar: cleaved caspase-3). Asterisks (*) on the bar graph indicate a statistically significant difference compared with the corresponding control (*$p < 0.05$, Mann-Whitney U test).

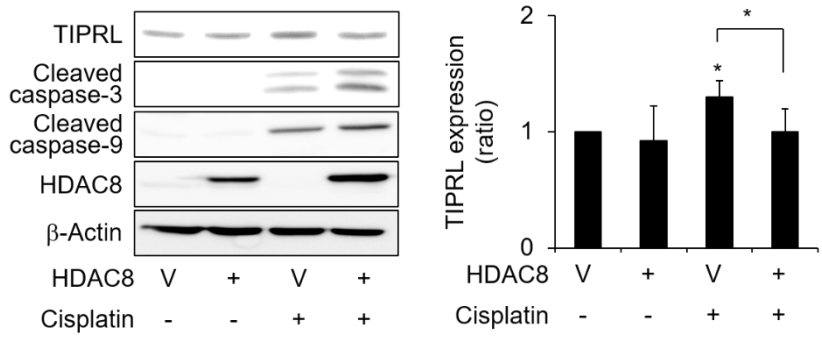

Figure 55. Effect of HDAC8 on TIPRL expression

For transient expression, H1299 cells were transfected with the pcDAN3.1(+) vector (V) and HDAC8 by lipofectamine for 24 h, and then cells were treated with 50 μM cisplatin for 48 h. Asterisks (*) on the bar graph indicate a statistically significant difference compared with the corresponding control (*$p < 0.05$, Mann-Whitney U test).

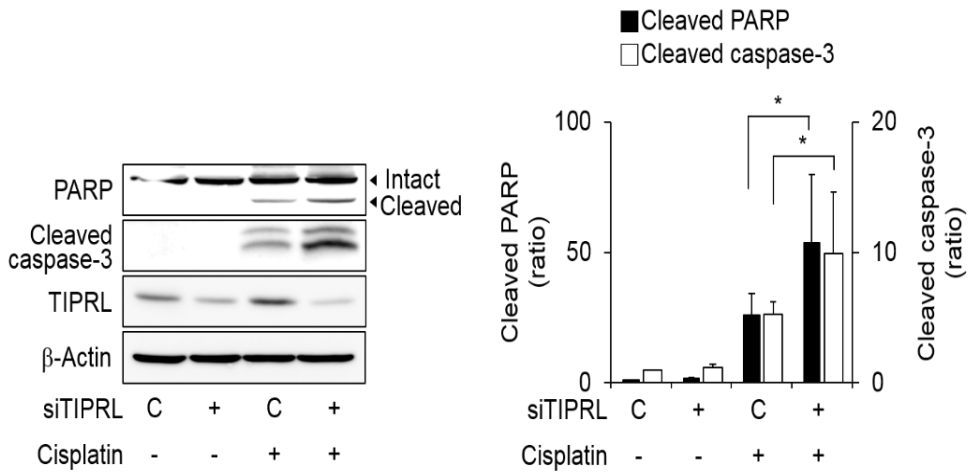

Figure 56. Effect of TIPRL on cisplatin–induced cleavage of PARP and caspase-3

For transient expression, H1299 cells were transfected with a control siRNA (C) or siTIPRL by lipofectamine for 24 h, and then cells were treated with 50 μM cisplatin for 48 h, and a subsequent western blot analysis (black bar: cleaved PARP, white bar: cleaved caspase-3). Asterisks (*) on the bar graph indicate a statistically significant difference compared with the corresponding control (*$p < 0.05$, Mann-Whitney U test).

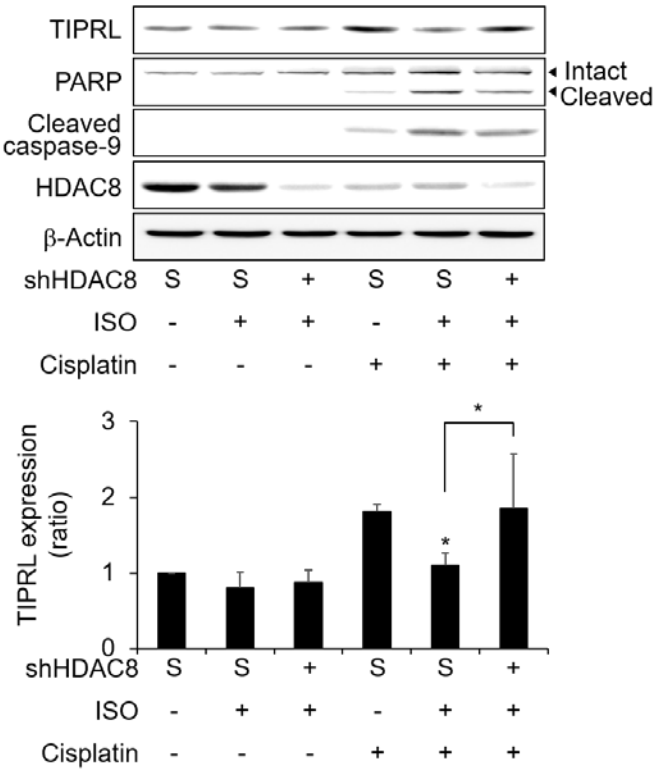

Figure 57. **Effect of shHDAC8 on isoproterenol-induced augmentation of apoptosis and TIPRL expression**

For transient expression, H1299 cells were transfected with a scrembled shRNA (S) or shHDAC8 #3 by lipofectamine for 24 h, and then cells were treated with 20 μM isoproterenol (ISO) for 30 min prior to 50 μM cisplatin treatment for 48 h, and a subsequent western blot analysis. Asterisks (*) on the bar graph indicate a statistically significant difference compared with the corresponding control (*p < 0.05, Mann-Whitney U test).

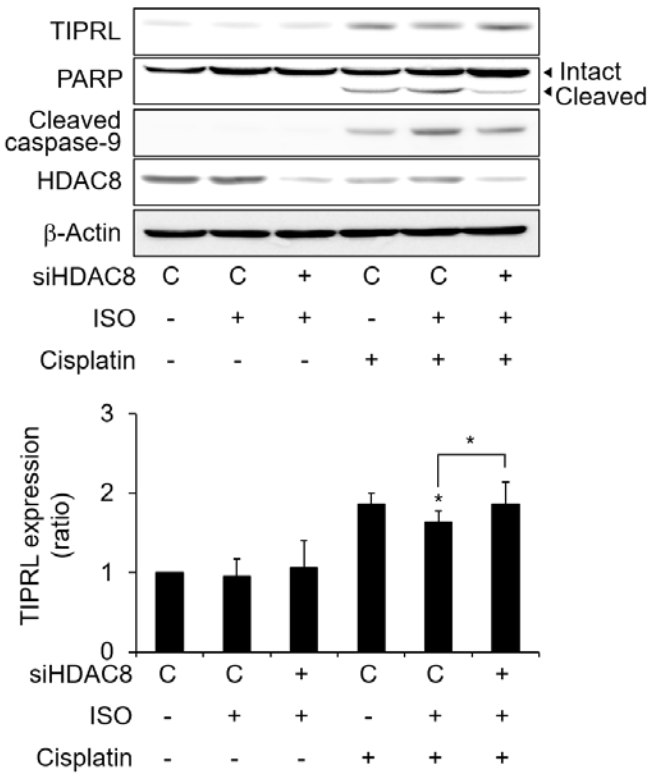

Figure 58. Effect of siHDAC8 on isoproterenol-induced augmentation of apoptosis and TIPRL expression

For transient expression, H1299 cells were transfected with a control siRNA (C) or siHDAC8 by lipofectamine for 24 h, and then cells were treated with 20 μM isoproterenol (ISO) for 30 min prior to 50 μM cisplatin treatment for 48 h and a subsequent western blot analysis. Asterisks (*) on the bar graph indicate a statistically significant difference compared with the corresponding control (*p < 0.05, Mann-Whitney U test).

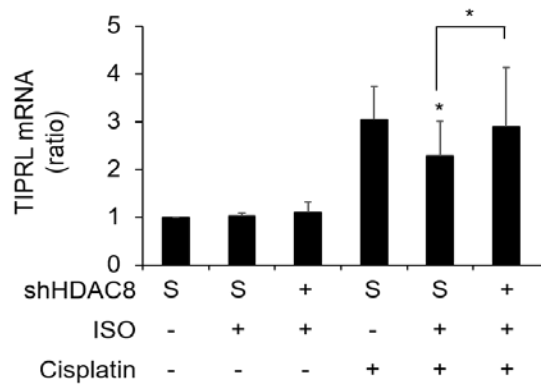

Figure 59. Effects of isoproterenol and HDAC8 on TIPRL mRNA levels in cisplatin-treated cells

For transient expression, H1299 cells were transfected with a scrembled shRNA (S) or shHDAC8 #3 by lipofectamine for 24 h, and then cells were treated with 20 μM isoproterenol (ISO) for 30 min prior to 50 μM cisplatin treatment for 48 h. TIPRL mRNA levels were analyzed by qRT-PCR. The amounts of TIPRL mRNA were normalized to the levels of GAPDH, and the results are presented as a ratio to the values of the untreated control. Asterisks (*) on the bar graph indicate a statistically significant difference compared with the corresponding control (*$p < 0.05$, Mann-Whitney U test).

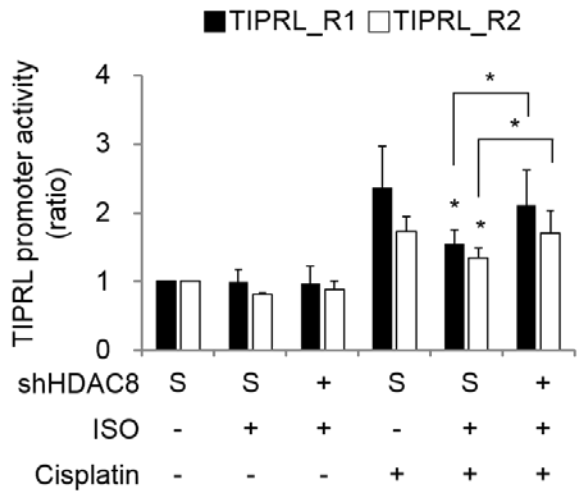

Figure 60. Effects of isoproterenol and HDAC8 on the promoter TIPRL activity in cisplatin-treated cells

H1299 cells were transfected with TIPRL-luciferase constructs (Renilla pLuc and TIPRL_R1-pLuc or TIPRL_R2-pLUc) and a scrambled shRNA (S) or shHDAC8 #3 by lipofectamine for 24 h, and then cells were treated with 20 μM isoproterenol (ISO) for 30 min prior to 50 μM cisplatin treatment for 24 h. TIPRL promoter activities were analyzed by Dual Luciferase System and normalized to renilla activity (black bar: TIPRL_R1, white bar: TIPRL_R2). Asterisks (*) on the bar graph indicate a statistically significant difference compared with the corresponding control (*p < 0.05, Mann-Whitney U test).

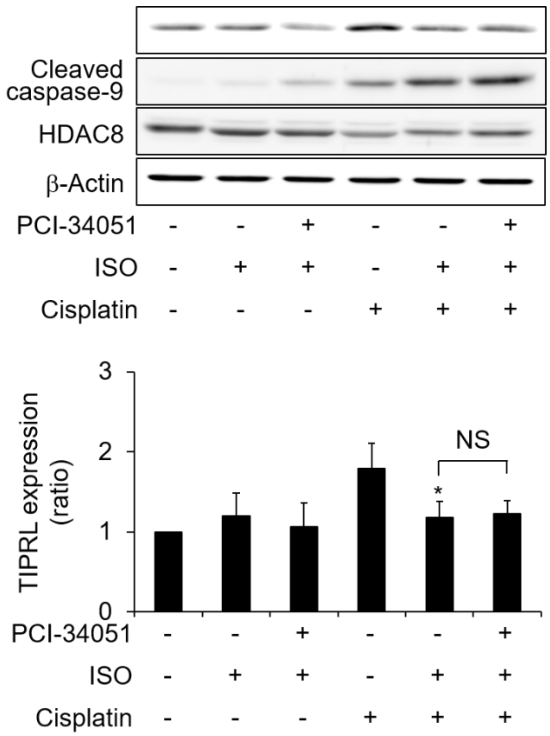

Figure 61. Effect of PCI-34051 on isoproterenol-induced augmentation of isoproterenol and HDAC8 on TIPRL expression

H1299 cells were sequentially treated with 10 μM PCI-34051 (HDAC8-specific inhibitor) for 24 h, 20 μM isoproterenol (ISO) for 30 min, and 50 μM cisplatin for 48 h before the western blot analysis. The asterisk (*) on the bar graph indicates a statistically significant difference compared with the corresponding control and NS indicates no statistically significant difference compared with the corresponding control (*$p < 0.05$, Mann-Whitney U test).

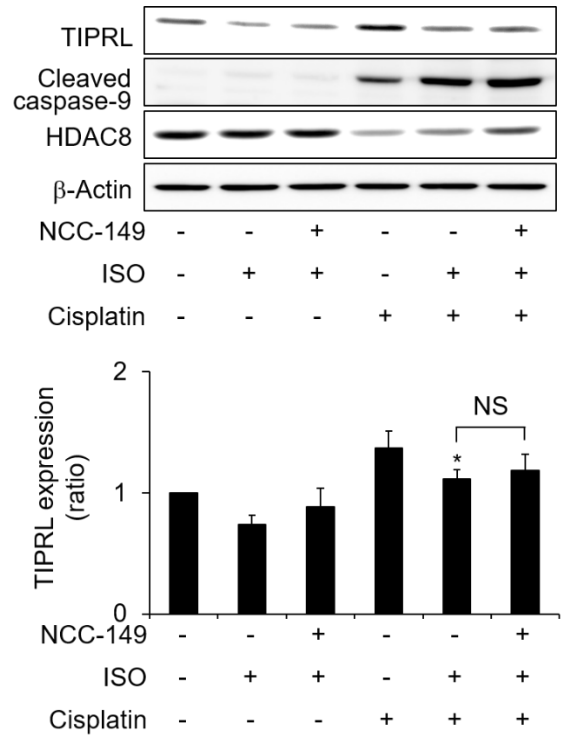

Figure 62. Effect of NCC-149 on isoproterenol-induced augmentation of isoproterenol and HDAC8 on TIPRL expression

H1299 cells were sequentially treated with 2 μM NCC-149 (HDAC8-specific inhibitor) for 24 h, 20 μM isoproterenol (ISO) for 30 min, and 50 μM cisplatin for 48 h before the western blot analysis. The asterisk (*) on the bar graph indicates a statistically significant difference compared with the corresponding control and NS indicates no statistically significant difference compared with the corresponding control (*$p < 0.05$, Mann-Whitney U test).

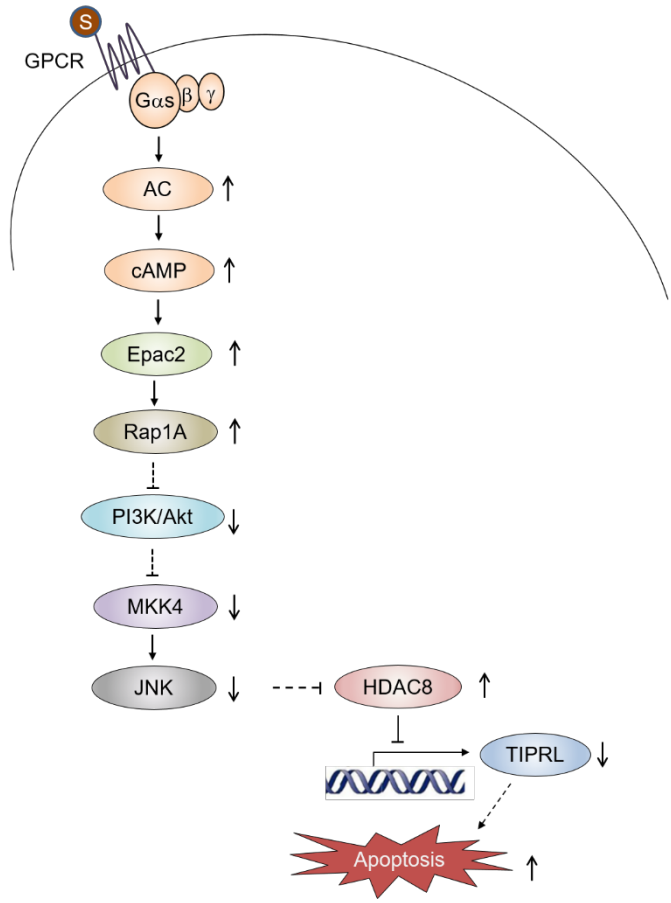

Figure 63. A suggested model for how increased HDAC8 expression by cAMP signaling system regulates cisplatin-induced apoptosis in H1299 cells

The solid lines indicate proven signaling pathways, and the dotted lines indicate suggested signaling pathways**.**

Discussion

This study was examined to determine the mechanism of how cAMP signaling system increase the HDAC8 expression and the effects on cisplatin-induced apoptosis and the underlying mechanisms in lung cancer cells. We found that the cAMP signaling system increases HDAC8 expression by inhibiting degradation of HDAC8 through Epac2-Rap1A-mediated inhibition of PI3K/Akt-JNK pathways, and that the cAMP signaling system augments cisplatin-induced apoptosis via the HDAC8-dependent repression of TIPRL expression in NSCLC cells (Fig. 64).

Our finding that the cAMP signaling system increases HDAC8 expression in lung cancer cells was supported by experiments showing that HDAC8 expression was increased after activation of cAMP signaling via expression of constitutively active Gαs or treatment with Gαs-coupled receptor agonists in H1299 and A549 NSCLC cells. The effect of cAMP signaling on HDAC8 expression seems HDAC8-specific, because the expression of other class I HDACs was not affected by the activation of cAMP signaling (data now shown). cAMP signaling regulates the nuclear localization of HDAC4 and HDAC5 [37, 38]. However, the effect of cAMP signaling on HDAC8 expression has not been reported, and to the best of our knowledge, we show for the first time in this paper that cAMP signaling increases HDAC8 expression in lung cancer cells. This finding, together with our recent report that cAMP signaling increases the HDAC6 expression [39], suggests that cAMP signaling might regulate protein acetylation by controlling HDACs expression and via the phosphorylation and localization of HDACs.

cAMP signaling system activates three major effector molecules: PKA, Epac and cyclic-nucleotide-gated ion channels, and these effectors regulate various cellular responses. This study revealed that Epac2 mediates HDAC8-increaseng effect of isoproterenol by demonstrating that the Epac-selective cAMP analog, 8-pCPT-cAMP, increased HDAC8 expression, and the Epac2 inhibition abolished the effect of isoproterenol on HDAC8 expression. However, the inhibition of either PKA or Epac1 did not abolish the effect of isoproterenol on HDAC8 expression, and the expression of a catalytic subunit of PKA did not increase HDAC8 expression, though it increased the phosphorylation of many proteins including CREB. PKA was reported to phosphorylate HDAC8, thereby reducing its activity in HeLa cervical cancer cells [16]. Therefore, it is possible that cAMP signaling could modulate HDAC8 activity either by inhibiting the phosphorylation of HDAC8 via PKA or by upregulating HDAC8 protein levels via Epac. However, the mechanism for the regulation of the two dichotic pathways of cAMP signaling is unclear and thus requires elucidation.

Epac plays a role as cAMP-regulated guanine nucleotide exchange factor for the Ras family members Rap1 and Rap2 [40, 41]. Epac proteins regulate a large number or cellular processes, including cell proliferation, differentiation, survival, and apoptosis; thus, alterations in Epac signaling have been implicated in the pathophysiology of numerous diseases including cancer and diseases of the heart, brain, and lung [42]. Epac activation was reported to induce the nuclear export of HDAC4 via a Ras-dependent signaling pathway and the phosphorylation of HDAC4 by calmodulin kinase II, suggesting its role in epigenetic regulation [38, 43, 44]. Epac1 and Epac2 differ in their respective molecular structures, tissue expressions,

subcellular localizations, and functions [45, 46]. This study shows a novel role of Epac2, the mediation of isoproterenol-induced increase in HDAC8 expression which confirms the differential roles of the two Epac isoforms.

Because Rap1 is a downstream molecule of Epac, we analyzed whether Rap1 mediates the isoproterenol-induced increase in HDAC8 expression, and found that Rap1A increased HDAC8 expression. Rap1A was activated by isoproterenol and 8-pCPT-cAMP, that activation increased HDAC8 expression, and the inhibition of Rap1A, which was caused by the expression of dominant-negative Rap1A or knockdown with shRNA targeting Rap1A, abolished the HDAC8-increasing effect of isoproterenol. The Rap proteins belong to the Ras family of small G proteins, and several Rap isoforms are expressed in mammals. Rap proteins are activated by Rap guanine nucleotide exchange factors, including Epacs. Several Rap1 and Rap2 isoforms are expressed in mammals, and Rap1 is specifically activated by Epac2-mediated cAMP signaling pathway [47, 48]. Rap proteins regulate various cellular functions, including cell proliferation, differentiation, and apoptosis [49]. However, the role of Rap in histone modification is unclear, so our finding that Rap1 mediates the increase in HDAC8 expression suggests that the Rap1 protein might play a role in epigenetic regulation by modulating histone acetylation.

Next, in this study to discover the signaling pathway acting downstream of Epac2-Rap1A, we found that cAMP signaling increases HDAC8 expression through Epac2-Rap1A-mediated inhibition of PI3K/Akt pathways in H1299 cells. This finding was supported by the results that isoproterenol and 8-pCPT-cAMP inhibited Akt activity via Rap1A, and that HDAC8 expression was increased when PI3K/Akt was inhibited by treatment with specific pharmacological inhibitors of PI3K and Akt or by

expression of dominant-negative PI3K and Akt. PI3K/Akt was reported to mediate the laminar flow-induced activation of histone deacetylases including HDAC8 in endothelial cells [50, 51]. However, the effect of Akt on HDAC8 expression has not yet been made clear, and our study presents a new role of PI3K/Akt: The regulation of HDAC8 expression. cAMP signaling has reportedly inhibited Akt activity by activating Epac and Rap1 in thyroid, glioma, and kidney cells [52-55]. However, Epac increases Akt activity in neuronal cells and human umbilical cord blood-derived mesenchymal stem cells [56, 57]. The differential effects of Epac2/Rap1 on Akt activation could provide a potential mechanism for cell type-specific effects in cAMP signaling [58].

The inhibition of Akt via treatment with isoproterenol caused a decrease in the inhibitory phosphorylation of GSK-3β at Ser-9 and thus activation of the enzyme. Thus, GSK-3β was assessed for whether it mediates the isoproterenol–induced increase in HDAC8 expression. However, the inhibition of GSK-3β activity with an inhibitor did not block the isoproterenol–induced increase in HDAC8 expression, indicating that isoproterenol increases HDAC8 expression in a GSK-3β-independent pathway. Thus, cAMP signaling seems to increase HDAC8 expression by inhibiting PI3K/Akt signaling via Epac2-Rap1A pathways.

This study also showed that isoproterenol increased HDAC8 expression by inhibiting the degradation of HDAC8 via autophagy and the ubiquitin-proteasome system. The finding is substantiated by the result that treatment with isoproterenol and forskolin/IBMX increased HDAC8 protein levels without increasing HDAC8 mRNA levels, and increased HDAC8 expression in the cells where protein biosynthesis was blocked with cycloheximide. Furthermore, the inhibition of either

proteasomal or lysosomal degradation by treatment with selective inhibitors increased the basal levels of HDAC8 protein, but abolished the increase in HDAC8 expression that was induced by isoproterenol and Akt inhibitor (MK-2206).

Proteins are degraded by the ubiquitin-proteasome system and lysosome system. HDAC8 protein was reportedly degraded by proteasome-mediated degradation following treatment with a proteasome inhibitor [59], but lysosomal degradation of HDAC8 has not yet been reported. The cAMP signaling system is known to regulate both the proteasomal degradation and lysosomal degradation of a variety of proteins. However, the specific degradation pathway involved in the cAMP-mediated HDAC8 degradation is unclear.

Next, we found that cAMP signaling inhibited autophagy-mediated HDAC8 degradation. This was confirmed by our finding that inhibiting of autophagy by treatment with 3-MA, autophagy inhibitor, increased HDAC8 expression. In addition, blocking the autophagy regulator by the expression of siRNA against Atg5 or Beclin1 also stimulated HDAC8 expression. The mammalian class III PI3K complex containing Vps34, Beclin1, and p150 plays a critical role in the initiation of autophagosome formation [60, 61]. Thus, the inhibition of class III PI3K and Beclin1 blocks the nucleation step of autophagy. Atg5 is conjugated to Atg12, and the Atg12-Atg5 conjugate then interacts noncovalently with Atg16L, which can act as an E3-like enzyme at the phagophore, an essential enzyme for autophagosomal elongation [62]. Therefore, the inhibition of Atg5 blocks the elongation step of autophagy. HDACs are involved in the regulation of autophagy and represent novel therapeutic targets for the modulation of the autophagic pathway. However, the mechanisms for the degradation of HDACs via autophagy are not clear. Our results

show that the inhibition of autophagy at the nucleation or elongation steps increased HDAC8 expression, demonstrating that HDAC8 is degraded via autophagy in H1299 cells. To the best of our knowledge, our study is the first to report that HDAC8 is degraded through the autophagy-lysosome system. This suggests that autophagy might be involved in the epigenetic regulation of gene expression by modulating HDACs.

Furthermore, the activation of the cAMP signaling system by the expression of constitutively active Gαs or by treatment with isoproterenol increased the expression of p62, and reduced conversion of LC3-I to LC3-II. Microtubule-associated protein 1 light chain 3 (LC3)/Atg8 and p62 are widely used as markers for autophagy [63]. The amount of LC3-II present is good marker for monitoring autophagosome formation and autophagic flux. The total cellular expression levels of protein p62 (also known as SQSTM1/sequestome 1) inversely correlate with autophagic activity. Therefore, the accumulation in p62 levels and the reduction in LC3-II levels caused by activation by cAMP signaling indicate that cAMP signaling inhibits autophagy in H1299 cells.

Next, we found that cAMP signaling decreased Bcl-2 phosphorylation. The inhibitory interaction of Bcl-2 on Beclin1 can be prevented by the phosphorylation of Bcl-2 at Ser-70 by stress-activated c-Jun N-terminal kinase 1 (JNK1) leading to the promotion of the autophagy-initiating complex [64]. Thus, the isoproterenol-induced decrease in Bcl-2 phosphorylation might reduce Beclin1 release from its inhibitory association with Bcl-2, which results in the inhibition of autophagy. cAMP signaling was reported to inhibit autophagy via Eapc-PLC-ε-IP3 and Ca^{2+}-calpain-Gαs mTOR-independent pathways, and isoproterenol can immediately inhibit

cardiac cellular autophagy [65-67]. Our study shows, for the first time to the best of our knowledge, that HDAC8 is degraded through the autophagy system and the autophagy of HDAC8 is inhibited by cAMP signaling system, which inhibits autophagy in H1299 cells.

This study showed that the cAMP signaling system increases HDAC8 protein levels by inhibiting the ubiquitin/proteasome-dependent degradation of HDAC8. This was confirmed by our findings that PYR-41, an E1 ubiquitin inhibitor, increased HDAC8 expression, and the ubiquitin E3 ligases Itch, MDM2, Skp2, and CHIP were involved in HDAC8 degradation in H1299 cells. However, only the phosphorylation of Itch was reduced by the cAMP signaling system. Itch, also known as atrophin-1-interacting protein 4 (AIP4), is a member of the Nedd4-like E3 ligase family of the HECT domain-containing E3 ubiquitin ligase group [68]. Itch activity is negatively regulated through intramolecular interactions in its unphosphorylated state, and these inhibitory interactions are removed after phosphorylation by JNK1 [69]. Thus, the reduction of Itch phosphorylation by isoproterenol treatment indicates that isoproterenol inhibits Itch activity.

In further experiments to study how the cAMP signaling system inhibits both the autophagy and the ubiquitin-proteasome system in H1299 cells, we found that cAMP signaling increased HDAC8 expression by inhibiting its degradation that involves JNK pathway, which regulates both phosphorylation of the Bcl-2 and Itch. Treatment with isoproterenol or forskolin/IMBX inhibited JNK activation and inhibiting JNK by either treatment with a JNK inhibitor or by the expression of dominant-negative JNK decreased the phosphorylation of both Bcl-2 and Itch. In addition, the activation of JNK by the expression of constitutively active JNK blocked the isoproterenol-

reduced activity of Bcl-2 and Itch. The JNK1-mediated phosphorylation of Bcl-2 dissociates Beclin1 from the inhibitory Bcl-2-Beclin1 complex and results in the activation of autophagy [64], and JNK1-mediated phosphorylation of Itch activates Itch to result in the activation of the ubiquitin-proteasome pathway [69]. These results indicate that cAMP signaling inhibits both the JNK-mediated phosphorylation of Bcl-2, thereby reducing autophagy, and the JNK-mediated phosphorylation of Itch, thereby reducing ubiquitin-proteasome-dependent degradation, resulting in increased HDAC8 protein levels.

To identify the pathway how cAMP signaling inhibits JNK, we analyzed the role of PI3K/Akt in this process. Inhibition of either PI3K or Akt activity decreased the phosphorylation of JNK. Akt regulates the two major intracellular proteolytic signaling pathways-ubiquitination and autophagy [70]-and is involved in the degradation of numerous proteins [71]. PI3K/Akt has been reported to mediate laminar flow-induced activation of histone deacetylases, including HDAC8, in endothelial cells [51], but the role of Akt on HDAC8 expression remained unclear. Our finding suggests the activation of MKK4/JNK, which is involved in controlling protein degradation, as a novel mechanism for Akt-mediated regulation of protein degradation. Activation of the JNK pathway by Akt, whereby inhibition of Akt activation blocks anti-5-methylchrysene-1,2-diol-3,4-epoxide (5-MCDE)-induced activation of JNKs in mouse epidermal cells, has been previously described [72]. However, the upstream signaling molecules for MKK4-mediated JNK activation by Akt are unknown. cAMP signaling regulates both the proteasomal and lysosomal degradation of various proteins. For example, cAMP-Epac1 signaling regulates the $ECS^{socs\text{-}3}$ E3 ubiquitin ligase complex to regulate cytokine signaling [73], and cAMP

signaling inhibits autophagy through the cAMP-Epac-phospholipase C pathway [67]. This study presents inhibition of the JNK pathway via Epac2-Rap1A-Akt as a novel pathway for cAMP signaling to regulate protein degradation in non-small cell lung cancer cells.

Finally, we examined the effect of increased HDAC8 expression on cisplatin-induced apoptosis and the underlying mechanism. We found that cAMP signaling augments cisplatin-induced apoptosis via the HDAC8-dependent repression of TIPRL expression in lung cancer cells. Experiments showed that 1) cAMP signaling augmented cisplatin- or γ-ray-induced apoptosis in H1299 lung cancer cells, 2) that cAMP signaling increased HDAC8 expression, 3) that exogenous expression of HDAC8 resulted in the augmentation of cisplatin-induced apoptosis, and 4) that knockdown of HDAC8 abolished the augmentation of apoptosis induced by cAMP signaling. Furthermore, the exogenous expression of HDAC8 reduced cisplatin-induced TIPRL expression, and the knockdown of TIPRL expression augmented the cisplatin-induced apoptosis. Finally, the knockdown of HDAC8 restored the cisplatin-induced TIPRL expression and abolished the isoproterenol-induced augmentation of apoptosis in cisplatin-treated H1299 cells. In addition, we found that cAMP signaling decreased the transcription of the TIPRL gene by increasing the HDAC8 expression. This founding is supported by the result that isoproterenol decreased the transcription of the TIPRL gene promoter and the mRNA level, and that knockdown of HDAC8 expression abolished the isoproterenol effect on TIPRL expression in cisplatin-treated cells.

β-adrenergic receptor agonists, including isoproterenol and epinephrine are known to improve sensitivity to cisplatin in NSCLC cells [74], and

cisplatin/epinephrine injectable gel has been shown to reduce solid tumor size in clinical trials [75]. In addition, we previously reported that the cAMP signaling augments cisplatin- or γ-ray-induced apoptosis by modulating the expression of Bcl-2 family proteins [31, 32], and the activation of ATM in lung cancer cells [33]. Here, we present a novel mechanism for how cAMP signaling modulates apoptosis: The repression of TIPRL expression by increasing HDAC8 expression. However, repression of TIPRL expression by HDAC8 appeared to be independent of HDAC8 deacetylase activity because pharmacological inhibition of the HDAC8 activity (PCI-34051 and NCC-149), in contrast to HDAC8 knockdown with shRNA or siRNA, did not block the isoproterenol-induced TIPRL repression or apoptotic augmentation. A similar effect for PCI-34051 on apoptosis was previously reported, whereby the PCI-34051-mediated inhibition of HDAC8 induced caspase-dependent apoptosis in cell lines that were derived from T-cell lymphomas or leukemias but not in other hematopoietic or solid tumor lines, including A549 lung cancer cells [21]. The mechanisms that drive the different outcomes for HDAC8 expression versus activity are unclear. Recently, HDAC8 is known to deacetylase the K(ac)20 site on the H4 histone tail, and catalyze deacetylation of p53 transcription factor [76]. Further studies are needed to explain the role of HDAC8 in catalyzing the deacetylation of TIPRL, and the mechanism of this differences.

TIPRL reportedly expresses higher levels in cancer tissues than normal tissues, and the knockdown of TIPRL augmented apoptosis by prolonging the MKK7/JNK activation triggered by TRAIL stimulation in hepatocellular carcinoma cell lines [36, 77]. These reports conform with our finding that the HDAC8-dependent repression of TIPRL expression by cAMP signaling contributes to the augmentation of

cisplatin-induced apoptosis. TIPRL is also reported to influence the phosphorylation state of a specific protein substrate of ataxia-telangiectasia mutated (ATM)- and Rad3-related (ATR) kinases, implying a role in DNA repair [78], which could also contribute to the modulation of apoptosis.

HDAC8 is also reportedly involved in the proliferation of lung cancer cells [79] and the invasion of breast cancer cells [80]; thus, the other biological effects of cAMP-induced increases in HDAC8 require further study.

Targeting cAMP signaling is vigorously investigated to develop novel approaches for the enhancement of therapeutic effects for various cancers, and many extensive research studies are performed on HDAC inhibitors to develop new anti-cancer drugs [81, 82]. Thus, this study might contribute to the development of new strategies to improve the efficiencies of chemotherapy and radiotherapy against cancers such as lung cancer by modulating the activity of cAMP signaling and HDACs.

In conclusion, the present study shows that the Epac-Rap1-Akt pathway mediates cAMP signaling-induced inhibition of JNK-dependent HDAC8 degradation, that the resulting increase in HDAC8 augments cisplatin-induced apoptosis by repressing TIPRL expression in H1299 lung cancer cells.

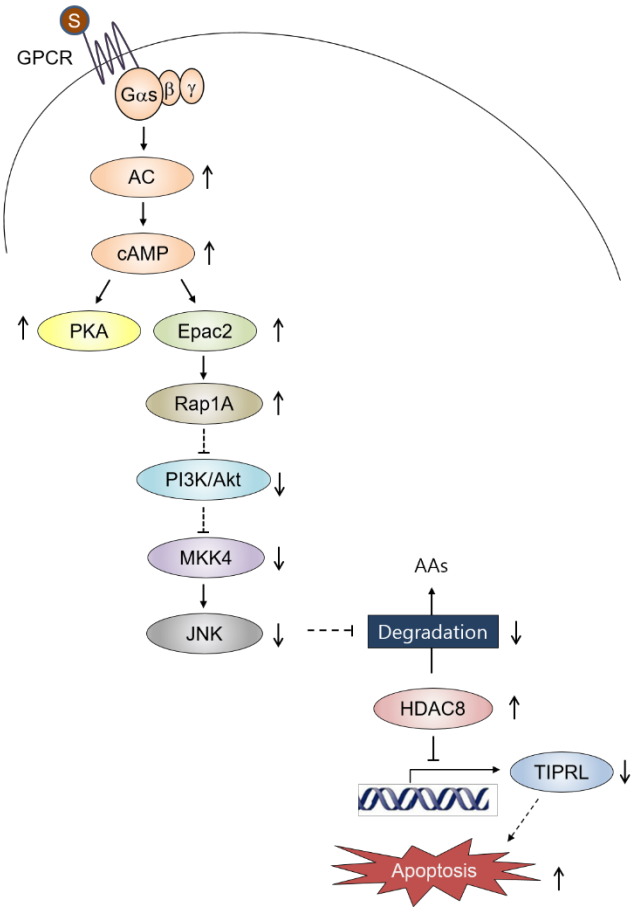

Figure 64. A proposed mechanism for the reduction of HDAC8 degradation by cAMP signaling system, which results in augmentation of apoptosis in NSCLC cells

The solid lines indicate proven signaling pathways, and the dotted lines indicate suggested signaling pathways**.**

Conclusion

From the results, the following conclusions were obtained.

1. cAMP signaling system increases HDAC8 expression by inhibiting HDAC8 degradation through Epac2-Rap1A-mediated inhibition of PI3K/Akt-JNK pathways in non-small cell lung cancer cells.

2. Increased HDAC8 expression by cAMP signaling augments cisplatin-induced apoptosis by repressing TIPRL expression in H1299 lung cancer cells.

These findings provide a novel mechanism of cAMP signaling system to regulate HDAC8 expression that modulates apoptosis of lung cancer cells and suggest that the cAMP signaling system can be utilized to enhance the therapeutic efficiency of treatments of lung cancers with cisplatin or radiation.

References

1. Fimia, G.M., and Sassone-Corsi, P. (2001). Cyclic AMP signalling. J Cell Sci *114*, 1971-1972.
2. Sassone-Corsi, P. (2012). The cyclic AMP pathway. Cold Spring Harb Perspect Biol *4*.
3. Gold, M.G., Gonen, T., and Scott, J.D. (2013). Local cAMP signaling in disease at a glance. J Cell Sci *126*, 4537-4543.
4. Kopperud, R., Krakstad, C., Selheim, F., and Døskeland, S.O. (2003). cAMP effector mechanisms. Novel twists for an 'old' signaling system. FEBS Letters *546*, 121-126.
5. Pertseva, M.N. (2000). [Hypothesis of the key coordinating role of adenylate cyclase signal mechanism and cAMP in regulatory effect of insulin superfamily peptides on fundamental cellular processes: cell growth, apoptosis, metabolism (Development of the L. G. Leibson's works)]. Zh Evol Biokhim Fiziol *36*, 494-503.
6. Cheng, X., Ji, Z., Tsalkova, T., and Mei, F. (2008). Epac and PKA: a tale of two intracellular cAMP receptors. Acta Biochim Biophys Sin (Shanghai) *40*, 651-662.
7. Oldenburger, A., Maarsingh, H., and Schmidt, M. (2012). Multiple facets of cAMP signalling and physiological impact: cAMP compartmentalization in the lung. Pharmaceuticals (Basel) *5*, 1291-1331.
8. Fajardo, A.M., Piazza, G.A., and Tinsley, H.N. (2014). The role of cyclic nucleotide signaling pathways in cancer: targets for prevention and

treatment. Cancers (Basel) *6*, 436-458.

9. Dorsam, R.T., and Gutkind, J.S. (2007). G-protein-coupled receptors and cancer. Nat Rev Cancer *7*, 79-94.

10. Saha, R.N., and Pahan, K. (2006). HATs and HDACs in neurodegeneration: a tale of disconcerted acetylation homeostasis. Cell Death Differ *13*, 539-550.

11. Yang, X.J., and Seto, E. (2003). Collaborative spirit of histone deacetylases in regulating chromatin structure and gene expression. Curr Opin Genet Dev *13*, 143-153.

12. de Ruijter, A.J., van Gennip, A.H., Caron, H.N., Kemp, S., and van Kuilenburg, A.B. (2003). Histone deacetylases (HDACs): characterization of the classical HDAC family. Biochem J *370*, 737-749.

13. Gao, L., Cueto, M.A., Asselbergs, F., and Atadja, P. (2002). Cloning and functional characterization of HDAC11, a novel member of the human histone deacetylase family. J Biol Chem *277*, 25748-25755.

14. Karagiannis, T.C., and Ververis, K. (2012). Potential of chromatin modifying compounds for the treatment of Alzheimer's disease. Pathobiol Aging Age Relat Dis *2*.

15. Buggy, J.J., Sideris, M.L., Mak, P., Lorimer, D.D., McIntosh, B., and Clark, J.M. (2000). Cloning and characterization of a novel human histone deacetylase, HDAC8. Biochem J *350 Pt 1*, 199-205.

16. Lee, H., Rezai-Zadeh, N., and Seto, E. (2003). Negative Regulation of Histone Deacetylase 8 Activity by Cyclic AMP-Dependent Protein Kinase A. Molecular and Cellular Biology *24*, 765-773.

17. Durst, K.L., Lutterbach, B., Kummalue, T., Friedman, A.D., and Hiebert, S.W. (2003). The inv(16) fusion protein associates with corepressors via a smooth muscle myosin heavy-chain domain. Mol Cell Biol *23*, 607-619.

18. Lee, H., Sengupta, N., Villagra, A., Rezai-Zadeh, N., and Seto, E. (2006). Histone deacetylase 8 safeguards the human ever-shorter telomeres 1B (hEST1B) protein from ubiquitin-mediated degradation. Mol Cell Biol *26*, 5259-5269.

19. Wilson, B.J., Tremblay, A.M., Deblois, G., Sylvain-Drolet, G., and Giguere, V. (2010). An acetylation switch modulates the transcriptional activity of estrogen-related receptor alpha. Mol Endocrinol *24*, 1349-1358.

20. West, A.C., and Johnstone, R.W. (2014). New and emerging HDAC inhibitors for cancer treatment. J Clin Invest *124*, 30-39.

21. Balasubramanian, S., Ramos, J., Luo, W., Sirisawad, M., Verner, E., and Buggy, J.J. (2008). A novel histone deacetylase 8 (HDAC8)-specific inhibitor PCI-34051 induces apoptosis in T-cell lymphomas. Leukemia *22*, 1026-1034.

22. Ropero, S., and Esteller, M. (2007). The role of histone deacetylases (HDACs) in human cancer. Mol Oncol *1*, 19-25.

23. Glozak, M.A., and Seto, E. (2007). Histone deacetylases and cancer. Oncogene *26*, 5420-5432.

24. Kroesen, M., Gielen, P., Brok, I.C., Armandari, I., Hoogerbrugge, P.M., and Adema, G.J. (2014). HDAC inhibitors and immunotherapy; a double edged sword? Oncotarget *5*, 6558-6572.

25. Wong, R.S. (2011). Apoptosis in cancer: from pathogenesis to treatment. J

Exp Clin Cancer Res *30*, 87.

26. Lowe, S.W., and Lin, A.W. (2000). Apoptosis in cancer. Carcinogenesis *21*, 485-495.

27. Elmore, S. (2007). Apoptosis: a review of programmed cell death. Toxicol Pathol *35*, 495-516.

28. Chipuk, J.E., and Green, D.R. (2006). Dissecting p53-dependent apoptosis. Cell Death Differ *13*, 994-1002.

29. Shivapurkar, N., Reddy, J., Chaudhary, P.M., and Gazdar, A.F. (2003). Apoptosis and lung cancer: a review. J Cell Biochem *88*, 885-898.

30. Pore, M.M., Hiltermann, T.J., and Kruyt, F.A. (2013). Targeting apoptosis pathways in lung cancer. Cancer Lett *332*, 359-368.

31. Choi, Y.J., Oh, J.M., Kim, S.Y., Seo, M., and Juhnn, Y.S. (2009). Stimulatory heterotrimeric GTP-binding protein augments cisplatin-induced apoptosis by upregulating Bak expression in human lung cancer cells. Cancer Sci *100*, 1069-1074.

32. Choi, Y.J., Kim, S.Y., Oh, J.M., and Juhnn, Y.S. (2009). Stimulatory heterotrimeric G protein augments gamma ray-induced apoptosis by up-regulation of Bak expression via CREB and AP-1 in H1299 human lung cancer cells. Exp Mol Med *41*, 592-600.

33. Cho, E.A., Kim, E.J., Kwak, S.J., and Juhnn, Y.S. (2014). cAMP signaling inhibits radiation-induced ATM phosphorylation leading to the augmentation of apoptosis in human lung cancer cells. Mol Cancer *13*, 36.

34. Komatsu, N., Kawamata, N., Takeuchi, S., Yin, D., Chien, W., Miller, C.W., and Koeffler, H.P. (2006). SAHA, a HDAC inhibitor, has profound anti-

growth activity against non-small cell lung cancer cells. Oncol Rep *15*, 187-191.

35. Seo, M., Cho, C.H., Lee, Y.I., Shin, E.Y., Park, D., Bae, C.D., Lee, J.W., Lee, E.S., and Juhnn, Y.S. (2004). Cdc42-dependent mediation of UV-induced p38 activation by G protein betagamma subunits. J Biol Chem *279*, 17366-17375.

36. Song, I.S., Jun, S.Y., Na, H.J., Kim, H.T., Jung, S.Y., Ha, G.H., Park, Y.H., Long, L.Z., Yu, D.Y., Kim, J.M., et al. (2012). Inhibition of MKK7-JNK by the TOR signaling pathway regulator-like protein contributes to resistance of HCC cells to TRAIL-induced apoptosis. Gastroenterology *143*, 1341-1351.

37. Ha, C.H., Kim, J.Y., Zhao, J., Wang, W., Jhun, B.S., Wong, C., and Jin, Z.G. (2010). PKA phosphorylates histone deacetylase 5 and prevents its nuclear export, leading to the inhibition of gene transcription and cardiomyocyte hypertrophy. Proc Natl Acad Sci U S A *107*, 15467-15472.

38. Liu, Y., and Schneider, M.F. (2013). Opposing HDAC4 nuclear fluxes due to phosphorylation by beta-adrenergic activated protein kinase A or by activity or Epac activated CaMKII in skeletal muscle fibres. J Physiol *591*, 3605-3623.

39. Lim, J.A., and Juhnn, Y.S. (2016). Isoproterenol increases histone deacetylase 6 expression and cell migration by inhibiting ERK signaling via PKA and Epac pathways in human lung cancer cells. Exp Mol Med *48*, e204.

40. de Rooij, J., Zwartkruis, F.J., Verheijen, M.H., Cool, R.H., Nijman, S.M., Wittinghofer, A., and Bos, J.L. (1998). Epac is a Rap1 guanine-nucleotide-

exchange factor directly activated by cyclic AMP. Nature *396*, 474-477.

41. Kawasaki, H., Springett, G.M., Toki, S., Canales, J.J., Harlan, P., Blumenstiel, J.P., Chen, E.J., Bany, I.A., Mochizuki, N., Ashbacher, A., et al. (1998). A Rap guanine nucleotide exchange factor enriched highly in the basal ganglia. Proc Natl Acad Sci U S A *95*, 13278-13283.

42. Schmidt, M., Dekker, F.J., and Maarsingh, H. (2013). Exchange protein directly activated by cAMP (epac): a multidomain cAMP mediator in the regulation of diverse biological functions. Pharmacol Rev *65*, 670-709.

43. Metrich, M., Laurent, A.C., Breckler, M., Duquesnes, N., Hmitou, I., Courillau, D., Blondeau, J.P., Crozatier, B., Lezoualc'h, F., and Morel, E. (2010). Epac activation induces histone deacetylase nuclear export via a Ras-dependent signalling pathway. Cell Signal *22*, 1459-1468.

44. Ohnuki, Y., Umeki, D., Mototani, Y., Jin, H., Cai, W., Shiozawa, K., Suita, K., Saeki, Y., Fujita, T., Ishikawa, Y., et al. (2014). Role of cyclic AMP sensor Epac1 in masseter muscle hypertrophy and myosin heavy chain transition induced by beta2-adrenoceptor stimulation. J Physiol *592*, 5461-5475.

45. Grandoch, M., Roscioni, S.S., and Schmidt, M. (2010). The role of Epac proteins, novel cAMP mediators, in the regulation of immune, lung and neuronal function. Br J Pharmacol *159*, 265-284.

46. Pereira, L., Rehmann, H., Lao, D.H., Erickson, J.R., Bossuyt, J., Chen, J., and Bers, D.M. (2015). Novel Epac fluorescent ligand reveals distinct Epac1 vs. Epac2 distribution and function in cardiomyocytes. Proc Natl Acad Sci U S A *112*, 3991-3996.

47. Li, Y., Asuri, S., Rebhun, J.F., Castro, A.F., Paranavitana, N.C., and Quilliam, L.A. (2006). The RAP1 guanine nucleotide exchange factor Epac2 couples cyclic AMP and Ras signals at the plasma membrane. J Biol Chem *281*, 2506-2514.

48. Shibasaki, T., Takahashi, H., Miki, T., Sunaga, Y., Matsumura, K., Yamanaka, M., Zhang, C., Tamamoto, A., Satoh, T., Miyazaki, J., et al. (2007). Essential role of Epac2/Rap1 signaling in regulation of insulin granule dynamics by cAMP. Proc Natl Acad Sci U S A *104*, 19333-19338.

49. Gloerich, M., Vliem, M.J., Prummel, E., Meijer, L.A., Rensen, M.G., Rehmann, H., and Bos, J.L. (2011). The nucleoporin RanBP2 tethers the cAMP effector Epac1 and inhibits its catalytic activity. J Cell Biol *193*, 1009-1020.

50. Zeng, L., Xiao, Q., Margariti, A., Zhang, Z., Zampetaki, A., Patel, S., Capogrossi, M.C., Hu, Y., and Xu, Q. (2006). HDAC3 is crucial in shear- and VEGF-induced stem cell differentiation toward endothelial cells. J Cell Biol *174*, 1059-1069.

51. Lee, D.Y., Lee, C.I., Lin, T.E., Lim, S.H., Zhou, J., Tseng, Y.C., Chien, S., and Chiu, J.J. (2012). Role of histone deacetylases in transcription factor regulation and cell cycle modulation in endothelial cells in response to disturbed flow. Proc Natl Acad Sci U S A *109*, 1967-1972.

52. Kim, S., Jee, K., Kim, D., Koh, H., and Chung, J. (2001). Cyclic AMP inhibits Akt activity by blocking the membrane localization of PDK1. J Biol Chem *276*, 12864-12870.

53. Lou, L., Urbani, J., Ribeiro-Neto, F., and Altschuler, D.L. (2002). cAMP

inhibition of Akt is mediated by activated and phosphorylated Rap1b. J Biol Chem *277*, 32799-32806.

54. Hong, K., Lou, L., Gupta, S., Ribeiro-Neto, F., and Altschuler, D.L. (2008). A novel Epac-Rap-PP2A signaling module controls cAMP-dependent Akt regulation. J Biol Chem *283*, 23129-23138.

55. Sugimoto, N., Miwa, S., Ohno-Shosaku, T., Tsuchiya, H., Hitomi, Y., Nakamura, H., Tomita, K., Yachie, A., and Koizumi, S. (2011). Activation of tumor suppressor protein PTEN and induction of apoptosis are involved in cAMP-mediated inhibition of cell number in B92 glial cells. Neurosci Lett *497*, 55-59.

56. Nijholt, I.M., Dolga, A.M., Ostroveanu, A., Luiten, P.G., Schmidt, M., and Eisel, U.L. (2008). Neuronal AKAP150 coordinates PKA and Epac-mediated PKB/Akt phosphorylation. Cell Signal *20*, 1715-1724.

57. Jang, M.W., Yun, S.P., Park, J.H., Ryu, J.M., Lee, J.H., and Han, H.J. (2012). Cooperation of Epac1/Rap1/Akt and PKA in prostaglandin E(2) -induced proliferation of human umbilical cord blood derived mesenchymal stem cells: involvement of c-Myc and VEGF expression. J Cell Physiol *227*, 3756-3767.

58. Mei, F.C., Qiao, J., Tsygankova, O.M., Meinkoth, J.L., Quilliam, L.A., and Cheng, X. (2002). Differential signaling of cyclic AMP: opposing effects of exchange protein directly activated by cyclic AMP and cAMP-dependent protein kinase on protein kinase B activation. J Biol Chem *277*, 11497-11504.

59. Li, Y., Li, X., and Guo, B. (2010). Chemopreventive agent 3,3'-diindolylmethane selectively induces proteasomal degradation of class I

histone deacetylases. Cancer Res *70*, 646-654.

60. Lamb, C.A., Yoshimori, T., and Tooze, S.A. (2013). The autophagosome: origins unknown, biogenesis complex. Nat Rev Mol Cell Biol *14*, 759-774.

61. Ravikumar, B., Sarkar, S., Davies, J.E., Futter, M., Garcia-Arencibia, M., Green-Thompson, Z.W., Jimenez-Sanchez, M., Korolchuk, V.I., Lichtenberg, M., Luo, S., et al. (2010). Regulation of mammalian autophagy in physiology and pathophysiology. Physiol Rev *90*, 1383-1435.

62. Janku, F., McConkey, D.J., Hong, D.S., and Kurzrock, R. (2011). Autophagy as a target for anticancer therapy. Nat Rev Clin Oncol *8*, 528-539.

63. Mizushima, N. (2010). Autophagy. FEBS Lett *584*, 1279.

64. Wei, Y., Pattingre, S., Sinha, S., Bassik, M., and Levine, B. (2008). JNK1-mediated phosphorylation of Bcl-2 regulates starvation-induced autophagy. Mol Cell *30*, 678-688.

65. Williams, A., Sarkar, S., Cuddon, P., Ttofi, E.K., Saiki, S., Siddiqi, F.H., Jahreiss, L., Fleming, A., Pask, D., Goldsmith, P., et al. (2008). Novel targets for Huntington's disease in an mTOR-independent autophagy pathway. Nat Chem Biol *4*, 295-305.

66. Pfeifer, U., Fohr, J., Wilhelm, W., and Dammrich, J. (1987). Short-term inhibition of cardiac cellular autophagy by isoproterenol. J Mol Cell Cardiol *19*, 1179-1184.

67. Fleming, A., Noda, T., Yoshimori, T., and Rubinsztein, D.C. (2011). Chemical modulators of autophagy as biological probes and potential therapeutics. Nat Chem Biol *7*, 9-17.

68. Melino, G., Gallagher, E., Aqeilan, R.I., Knight, R., Peschiaroli, A., Rossi,

M., Scialpi, F., Malatesta, M., Zocchi, L., Browne, G., et al. (2008). Itch: a HECT-type E3 ligase regulating immunity, skin and cancer. Cell Death Differ *15*, 1103-1112.

69. Gallagher, E., Gao, M., Liu, Y.C., and Karin, M. (2006). Activation of the E3 ubiquitin ligase Itch through a phosphorylation-induced conformational change. Proc Natl Acad Sci U S A *103*, 1717-1722.

70. Noguchi, M., Hirata, N., and Suizu, F. (2014). The links between AKT and two intracellular proteolytic cascades: ubiquitination and autophagy. Biochim Biophys Acta *1846*, 342-352.

71. Heras-Sandoval, D., Perez-Rojas, J.M., Hernandez-Damian, J., and Pedraza-Chaverri, J. (2014). The role of PI3K/AKT/mTOR pathway in the modulation of autophagy and the clearance of protein aggregates in neurodegeneration. Cell Signal *26*, 2694-2701.

72. Li, D.Q., Chen, Z., Song, X.J., Luo, L., and Pflugfelder, S.C. (2004). Stimulation of matrix metalloproteinases by hyperosmolarity via a JNK pathway in human corneal epithelial cells. Invest Ophthalmol Vis Sci *45*, 4302-4311.

73. Williams, J.J., and Palmer, T.M. (2012). Unbiased identification of substrates for the Epac1-inducible E3 ubiquitin ligase component SOCS-3. Biochem Soc Trans *40*, 215-218.

74. Bando, T., Fujimura, M., Kasahara, K., Shibata, K., Shirasaki, H., Heki, U., Iwasa, K., Ueda, A., Tomikawa, S., and Matsuda, T. (1997). Stimulation of beta-adrenoceptor enhances sensitivity to cisplatin in non-small cell lung cancer cell lines. Int J Oncol *10*, 1197-1201.

75. Malhotra, H., and Plosker, G.L. (2001). Cisplatin/epinephrine injectable gel. Drugs Aging *18*, 787-793; discussion 794-785.

76. Wolfson, N.A., Pitcairn, C.A., and Fierke, C.A. (2013). HDAC8 substrates: Histones and beyond. Biopolymers *99*, 112-126.

77. Lee, H.J., Cho, H.S., Jun, S.Y., Lee, J.J., Yoon, J.Y., Lee, J.H., Song, H.H., Choi, S.H., Kim, S.Y., Saloura, V., et al. (2014). Tussilago farfara L. augments TRAIL-induced apoptosis through MKK7/JNK activation by inhibition of MKK7TIPRL in human hepatocellular carcinoma cells. Oncol Rep *32*, 1117-1123.

78. McConnell, T.L., and Wetmore, S.D. (2007). How do size-expanded DNA nucleobases enhance duplex stability? Computational analysis of the hydrogen-bonding and stacking ability of xDNA bases. J Phys Chem B *111*, 2999-3009.

79. Vannini, A., Volpari, C., Filocamo, G., Casavola, E.C., Brunetti, M., Renzoni, D., Chakravarty, P., Paolini, C., De Francesco, R., Gallinari, P., et al. (2004). Crystal structure of a eukaryotic zinc-dependent histone deacetylase, human HDAC8, complexed with a hydroxamic acid inhibitor. Proc Natl Acad Sci U S A *101*, 15064-15069.

80. Park, S.Y., Jun, J.A., Jeong, K.J., Heo, H.J., Sohn, J.S., Lee, H.Y., Park, C.G., and Kang, J. (2011). Histone deacetylases 1, 6 and 8 are critical for invasion in breast cancer. Oncol Rep *25*, 1677-1681.

81. Lakshmaiah, K.C., Jacob, L.A., Aparna, S., Lokanatha, D., and Saldanha, S.C. (2014). Epigenetic therapy of cancer with histone deacetylase inhibitors. J Cancer Res Ther *10*, 469-478.

82. Vendetti, F.P., and Rudin, C.M. (2013). Epigenetic therapy in non-small-cell lung cancer: targeting DNA methyltransferases and histone deacetylases. Expert Opin Biol Ther *13*, 1273-1285.

국문 초록

cAMP 신호전달계가 폐암세포주에서 HDAC8 단백질분해를 조절하는 기전

박 지 연
의과학과 의과학전공
서울대학교 대학원

히스톤 탈아세틸화 효소 (HDAC)는 히스톤과 다른 단백질로부터 아세틸기를 제거하고 유전자 발현의 후성적 조절을 수행하는 역할을 한다. 고리형 아데노신 일인산 (cyclic AMP, cAMP) 신호전달계는 다양한 외부 신호 자극으로 형성된 cAMP 에 의해서 활성화되며, 유전자 발현, 증식, 사멸을 포함하는 다양한 세포의 기능을 조절한다. 하지만 cAMP 신호전달계가 HDAC의 발현에 미치는 영향에 관해서는 연구가 많이 이루어지지 않았다. 이 연구에서는 cAMP 신호전달계가 비소 폐암 세포주에서 히스톤 아세틸화 8 (HDAC8) 발현을 증가시키는 분자 기전과 증가한 HDAC8 발현이 세포사멸에는 어떠한 영향을 미치는가에 대해 연구를 하였다.

Isoproterenol 또는 prostaglandin E2 (PGE2)에 의한 cAMP 신호전달계의 활성화는 HDAC8 의 발현을 증가시켰다. Epac activator 인 8-pCPT-cAMP 를 처리 시에도 HDAC8 발현이 증가했다. Epac2 를 억제하게 되면 isoproterenol

에 의한 HDAC8 발현 증가를 막았지만 PKA 나 Epac1 을 억제하게 되면 isoproterenol 효과를 막지 못했다. Isoproterenol 과 8-pCPT-cAMP 는 Rap1 을 활성화 시켰고 Rap1A 활성화는 HDAC8 발현을 증가시켰다. 더욱이, Rap1A 의 억제는 isoproterenol 에 의해 유도된 HDAC8 발현의 증가를 막았다. Isoproterenol 은 Rap1A 의 활성화에 의해 Akt 를 억제하였고, PI3K/Akt 활성 억제는 MKK4/JNK 활성을 억제하고 HDAC8 발현을 증가시켰다. cAMP 신호전달계의 활성화는 HDAC8 mRNA 의 증가 없이 HDAC8 단백질 발현을 증가시켰다. Proteasomal 또는 lysosoaml 분해의 억제는 isoproterenol 또는 Akt 억제제에 의한 HDAC8 발현 증가를 막았다. cAMP 의 활성화는 autophagy 와 ubiquitin-proteasome 시스템 억제를 통해 HDAC8 분해를 억제하였다. cAMP 신호전달계는 JNK 활성 억제를 통하여 Bcl-2 및 Itch 의 인산화를 감소시킴으로써 autophagy 와 ubiquitin-proteasome 시스템 활성을 감소시켰다. Isoproterenol 은 HDAC8 발현을 증가시킴으로써 시스플라틴에 의해 유도된 세포 사멸을 증가시켰다. HDAC8 을 과발현하면 시스플라틴에 의해 유도된 TIPRL 발현을 감소시켰고, TIPRL 발현의 knockdown 은 시스플라틴에 의해 유도된 세포 사멸을 증가시켰다. HDAC8 을 knockdown 하면 시스플라틴에 의해 유도된 TIPRL 발현을 회복시켰고 isoproterenol 에 의해 유도된 세포 사멸의 증가를 저해했다. Isoproterenol 은 HDAC8 발현을 증가시킴으로써 TIPRL 유전자 전사를 감소시켰다. 이 연구를 통하여, 비소 폐암 세포에서 cAMP 신호전달계는 Epac2-Rap1A 거쳐 PI3K/Akt-JNK 활성 저해를 통한 단백질 분해를 억제함으로써 HDAC8 발현을 증가시키고, 증가된

HDAC8 발현은 TIPRL 발현 억제를 통해 시스플라틴에 의해 유도된 세포 사멸을 증가시킨다는 결론을 얻었다.

주요어 : cAMP 신호전달계, 히스톤 아세틸화 8 (HDAC8), 폐암, Akt, autophagy, JNK, ubiquitin-proteasome degradation
학 번 : 2011-30627